ELSEVIER

Available online at www.sciencedirect.com

ScienceDirect

Journal of the European Ceramic Society 29 (2009) 969–993

ECERS

www.elsevier.com/locate/jeurceramsoc

Review

Laser machining of structural ceramics—A review

Anoop N. Samant, Narendra B. Dahotre *

Department of Materials Science Engineering, The University of Tennessee, Knoxville, TN 37996, United States

Received 24 July 2008; received in revised form 11 November 2008; accepted 13 November 2008
Available online 6 January 2009

Abstract

Outstanding mechanical and physical properties like high thermal resistance, high hardness and chemical stability have encouraged use of structural ceramics in several applications. The brittle and hard nature of these ceramics makes them difficult to machine using conventional techniques and damage caused to the surface while machining affects efficiency of components. Laser machining has recently emerged as a potential technique for attaining high material removal rates. This review paper aims at presenting the state of the art in the field of laser machining of structural ceramics and emphasizes on experimental and computational approaches in understanding physical nature of the complex phenomena.
© 2008 Elsevier Ltd. All rights reserved.

Keywords: SiC; Al_2O_3; MgO; Si_3N_4; Traditional ceramics

Contents

1. Introduction 970
2. Fabrication techniques 970
 2.1. Mechanical machining 970
  2.1.1. Abrasive machining/grinding 970
  2.1.2. Ultrasonic machining (USM) 971
  2.1.3. Abrasive water jet machining (AWJM) 971
 2.2. Chemical machining (CM) 971
  2.2.1. Chemical–mechanical machining (CMM) 971
 2.3. Electrical machining 971
  2.3.1. Electrochemical machining (ECM) 971
  2.3.2. Electrical-discharge machining (EDM) 972
  2.3.3. Electro-chemical discharge machining (ECDM) 972
 2.4. Radiation machining 972
  2.4.1. Electron beam machining (EBM) 972
  2.4.2. Plasma arc machining 972
  2.4.3. Laser machining (LM) 972
 2.5. Hybrid machining 972
  2.5.1. Electrical discharge grinding 972
  2.5.2. Laser-assisted chemical etching 972
  2.5.3. Laser assisted machining (LAM) 972
3. Laser machining 973
 3.1. Absorption of laser energy and multiple reflections 974
 3.2. Thermal effects 975
  3.2.1. Melting and sublimation 976

* Corresponding author. Tel.: +1 865 974 3609; fax: +1 865 974 4115.
E-mail address: ndahotre@utk.edu (N.B. Dahotre).

0955-2219/$ – see front matter © 2008 Elsevier Ltd. All rights reserved.
doi:10.1016/j.jeurceramsoc.2008.11.010

3.2.2. Vaporization and dissociation 977
3.2.3. Plasma formation 977
3.2.4. Ablation 978
3.3. Types of machining 979
3.3.1. One-dimensional laser machining 980
3.3.2. Two-dimensional laser machining 980
3.3.3. Three-dimensional laser machining 980
4. State of the art 981
4.1. Alumina 981
4.2. Silicon nitride 984
4.3. Silicon carbide 985
4.4. Aluminum nitride 986
4.5. Zirconia 987
4.6. Magnesia 988
5. Laser micromachining 990
6. Conclusion 990
References 990

1. Introduction

Structural materials can be classified as ceramics, metals or polymers with each type of material having its own advantages and drawbacks. Even though metals are strong, cheap and tough, they are chemically reactive, heavy and have limitations on the maximum operating temperature. Polymers are easy to fabricate and light, but they can be used at temperatures only below 300 °C. The characteristic features of ceramics compared to others make them more suitable for some applications. In comparison with metals and polymers, most ceramics possess useful features such as high-temperature strength, superior wear resistance, high hardness, lower thermal and electrical conductivity and chemical stability.[1] Retention of these properties by structural ceramics at high temperatures presents these materials as an exclusive solution to several engineering application problems.[2] Commonly used structural ceramics are zirconia (ZrO_2), boron carbide (B_4C), alumina (Al_2O_3), silicon carbide (SiC), silicon nitride (Si_3N_4), sialon (Si–Al–O–N), berylia (BeO), magnesia (MgO), titanium carbide (TiC), titanium nitride (TiN), titanium diboride (TiB_2), zirconium nitride (ZrN) and zirconium diboride (ZrB_2). In general, these structural ceramics fall into two major groups: conductive ceramics such as carbides (TiC and SiC), borides (TiB_2 and ZrB_2) or nitrides (TiN and ZrN) and ceramics that are a mixture of dielectric (semi-conductive) materials and electrically conductive materials such as Si_3N_4–TiN, sialon-TiN, and Si_3N_4–SiC.[3] The applications of some of the structural ceramics are presented in Table 1 below.

Alumina is also used in making machine tool inserts, heat-resistant packings, electrical and electronic components and attachments to melting ducts and refractory linings.[4] Zirconium diboride (ZrB_2) possesses a high melting point, low density, and excellent resistance to thermal shock and oxidation compared to other non-oxide structural ceramics. Hence, it is used as an ultra-high-temperature ceramic (UHTC), for refractory materials and as electrodes or crucible materials.[5] Magnesia is a very stable oxide used in refractory linings, brake linings, thin-film semi-conductors, for housing thermocouples in aggressive environments, in making crucibles in chemical and nuclear industry where high corrosion resistance is required and in making thin-film substrates and laser parts.[6,7] In addition to the above-mentioned structural ceramics and their engineering applications, there are several other fields where these ceramics are significantly used. As applications of structural ceramics are not the main focus of this study, they will not be discussed in further detail here. These advanced high-performance materials have certain limitations such as difficulty in fabrication, high cost, and poor reproducibility as seen below.

2. Fabrication techniques

Many features (high hardness) that make structural ceramics attractive for particular uses also make them difficult to fabricate by traditional methods based on mechanical grinding and machining. Strength and efficiency of the components can be affected by the damage caused on the surface of the ceramics machined by conventional methods. A crucial step in manufacturing ceramic components is their cost-effective machining with excellent quality. Massive research efforts have been conducted on the precision machining of ceramic components over the past few decades, developing several advanced machining technologies without affecting the beneficial properties of the surface.[2] Some of these techniques are summarized in Fig. 1 and briefly described below.

2.1. Mechanical machining

In mechanical machining, material removal takes place when the ceramic is subjected to some mechanical force/impingement of abrasive particles. Commonly used techniques under this category are abrasive machining/grinding, ultrasonic machining, and abrasive water jet machining.

2.1.1. Abrasive machining/grinding

The machining takes place by using grinding wheels that are bonded abrasives used for producing several complex shapes.[8]

Table 1
Applications of different structural ceramics[1].

Application	Performance advantages	Examples
Wear parts: seals, bearings, valves, nozzles	High hardness, low friction	SiC, Al_2O_3
Cutting tools	High strength, hardness	Si_3N_4
Heat engines: diesel components, gas turbines	Thermal insulation, high-temperature strength, fuel economy	ZrO_2, SiC, Si_3N_4
Medical implants: hips, teeth, joints	Biocompatibility, surface bond to tissue, corrosion resistance	Hydroxyapatite, bioglass, Al_2O_3, ZrO_2
Construction: highways, bridges, buildings	Improved durability, lower overall cost	Advanced cements and concrete

Even though the needs for dimensional accuracy and surface finish are satisfied by conventional grinding, long machining times and high machining costs account for 60–90% of the final cost of the finished product. This poses a major hindrance for the grinding process[9,10] and ground products also generate surface and subsurface cracks,[11,12] pulverization layers,[13] some plastic deformation[14] and significant residual stresses.[15]

2.1.2. Ultrasonic machining (USM)

Ultrasonically vibrated abrasive particles remove material in ultrasonic machining at generally low material removal rates. A transducer/booster combination converts electrical energy into mechanical vibrations and causes the tool to vibrate along its longitudinal axis at high frequency.[16] As the mechanism of material removal is not properly documented, process optimization is difficult.[17]

2.1.3. Abrasive water jet machining (AWJM)

In abrasive water jet machining, a blast of abrasive-laden water stream impinges on the surface of the material and results in erosive wear. This process is advantageous over the grinding process as it reduces tool wear and machining time.[18] At high speeds, surface fracture results in kerf formation because of the hydrodynamic forces within the water jet.

2.2. Chemical machining (CM)

Chemical machining using etchants is the oldest of the machining processes, wherein chemicals attack the materials and remove small amounts from the surface. Sharp corners, deep cavities and porous workpieces cannot be easily machined as this method is only suitable for shallow removal of material (up to 12 mm).[8]

2.2.1. Chemical–mechanical machining (CMM)

This technology is widely used in surface patterning in semiconductors and micro-electro-mechanical systems (MEMS). Initially, the chemical absorption on the surface of the material produces a chemically reacted layer with physical properties different from the original material. This is followed by mechanical machining to generate the desired pattern on the surface. High costs and several steps involved in patterning commonly used materials such as silicon can be minimized by using KOH solution that can change hard brittle material surface of silicon into a hydrated layer which makes machining easier. Furthermore, this technique also offers flexibility and controllability in the process.[19]

2.3. Electrical machining

Electrical energy in the form of pulse or continuous in isolation or in combination with chemicals is used to erode the material. It is highly effective for machining electrically conductive and semi-conductive materials. Electrochemical machining (ECM), electrical-discharge machining (EDM) and electrochemical discharge machining (ECDM) are the commonly used electrical machining techniques.

2.3.1. Electrochemical machining (ECM)

Electrochemical machining is the reverse of electroplating used for machining complex cavities in high-strength materials. As the electrolyte has a tendency to erode away sharp profiles, this method is not suitable for generating sharp corners.

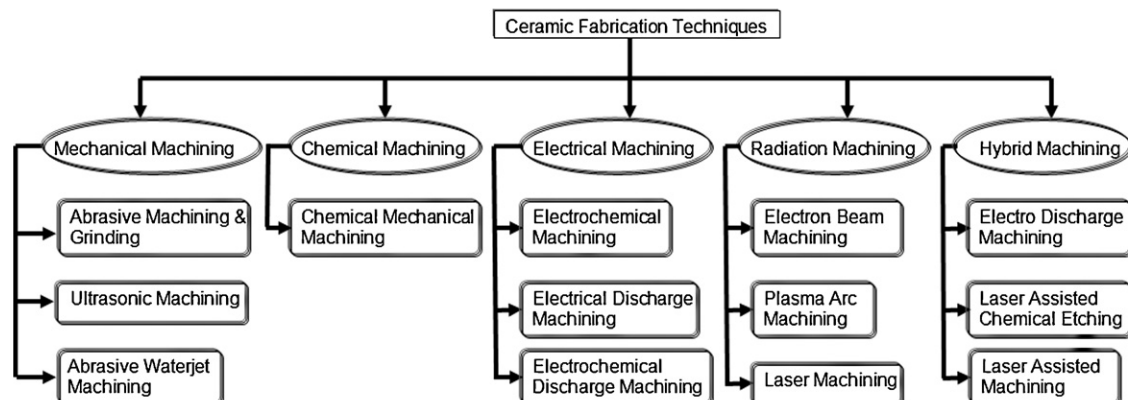

Fig. 1. Ceramic fabrication techniques.

2.3.2. Electrical-discharge machining (EDM)

EDM is an abrasionless method used for machining conductive ceramics such as boron carbide (B_4C) and silicon carbide (SiC).[20] This method is not affected by the hardness of the material, but requires an electrical resistivity of less than 100 Ω cm.[2]

2.3.3. Electro-chemical discharge machining (ECDM)

This technique has the combined features of EDM and ECM and is capable of machining high strength electrically non-conductive ceramics. This process is inefficient because a significant portion of the total heat developed is dissipated for increasing the temperature and the corresponding material removed while machining is less.[21]

2.4. Radiation machining

Radiation machining is a non-contact machining process where the dimension of the hole or the groove can be controlled by the energy supply to the work piece. The energy can be provided by an electron beam, plasma arc or by lasers. These non-contact machining techniques are not affected by the abrasion of the tools and they are independent of electrical resistivity of the materials being machined.

2.4.1. Electron beam machining (EBM)

The energy source in EBM is high-speed electrons that strike the surface of the work piece generating heat.[8] Since the beam can be positioned rapidly by a deflection coil, high machining speeds are possible. This machining process has the drawback that the width of the machined cavity increases while machining at high speeds due to the beam defocusing effect.[22]

2.4.2. Plasma arc machining

Ionized gas is used for machining the ceramic at very high temperatures leading to smaller kerf widths and good surface finish. As the vacuum chambers have limited capacity, the size of the components should closely match the size of the vacuum chamber.[8]

2.4.3. Laser machining (LM)

The source of energy in LM is a laser (acronym for Light Amplification by Stimulated Emission of Radiation). High density optical energy is incident on the surface of the work piece and the material is removed by melting, dissociation/decomposition (broken chemical bonds causes the material to dissociate/decompose), evaporation and material expulsion from the area of laser–material interaction. The vital parameters governing this process are the different properties of the ceramic such as reflectivity, thermal conductivity, specific heat and latent heats of melting and evaporation. The schematic representation of the laser machining process is made in Fig. 2. Laser machining of structural ceramics and the associated physical phenomena will be discussed extensively in the later part of this review.

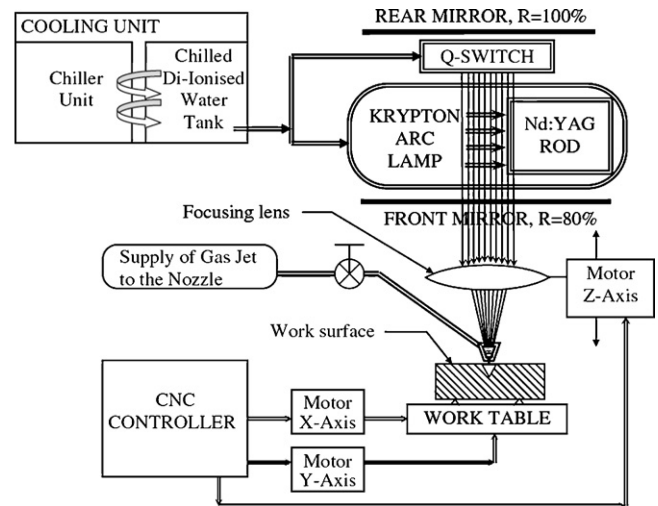

Fig. 2. Schematic of laser machining. (After Kuar et al.[23] with permission. Copyright Elsevier.)

2.5. Hybrid machining

Hybrid machining uses a combination of two or more of the above techniques for machining the ceramic such as electrical discharge grinding, laser-assisted chemical etching and machining using lasers and cutting tool/laser assisted machining (LAM).

2.5.1. Electrical discharge grinding

This method combining the advantages of grinding and electrical-discharge machining has low equipment cost and high efficiency.[24,25] Material is removed from the ceramic surface by recurring spark discharges between the rotating wheel and the work piece.[8]

2.5.2. Laser-assisted chemical etching

Material removal is carried out by using suitable etchant in combination with selective laser irradiation. The laser radiation influences the reaction between the material and the etchant by exciting the etchant molecules and/or the material surface[26] and the etch rate is significantly affected by the laser fluence.

2.5.3. Laser assisted machining (LAM)

In laser assisted machining, the material is locally heated by an intense laser source prior to material removal, without melting or sublimation of the ceramic. This technique has been successfully used for machining silicon nitride and the corresponding work piece temperature, tool wear and surface integrity have been measured.[27–32] Magnesia-partially-stabilized zirconia was machined with a polycrystalline cubic boron nitride tool and it was found that the tool life increased with material removal temperatures.[33] LAM effectively reduced the cutting force and improved the surface finish of the finished products made from Al_2O_3.[34] In LAM, after the laser is used to change the ceramic deformation behavior from brittle to ductile, material removal takes place with a conventional cutting tool. Unlike LAM, in laser machining (LM), actual material removal takes place by

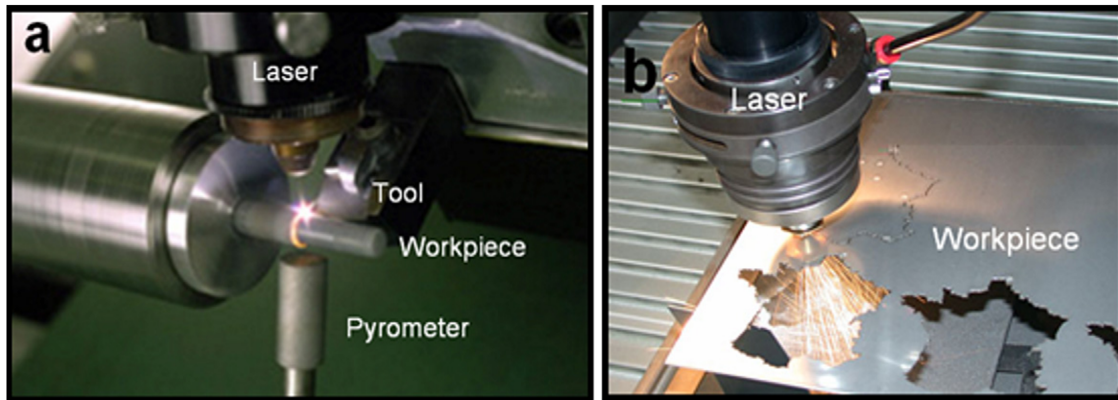

Fig. 3. (a) Laser assisted machining. (After Lei et al.[32] with permission. Copyright Elsevier.) (b) Laser machining.[35]

the laser beam. The physical phenomena taking place during the LAM of structural ceramics is different from LM and will not be a part of this study. The difference in the two processes is demonstrated in Fig. 3.

3. Laser machining

Lasers can replace mechanical material removal methods in several engineering applications because of their following salient features:[36]

(i) Non-contact process: Energy transfer from the laser to the ceramic through irradiation eliminates cutting forces, tool wear and machine vibration. Furthermore, the material removal rate is not affected by the maximum tool force, tool chatter or built-up edge formation, but can be controlled by varying the laser processing parameters such as input energy and processing speed.

(ii) Thermal process: The efficiency of laser machining depends on the thermal and, to some extent on the optical properties of the material. This makes hard or brittle materials such as structural ceramics with low thermal diffusivity and conductivity suitable for machining.

(iii) Flexible process: In combination with a multi-axis positioning system or robot, lasers can be used for drilling, cutting, grooving, welding and heat treating on the same machine without any necessity to transport the parts for processing them with specialized machines. In-process monitoring during the laser machining process can allow key parameters to be measured and a high level of reproducibility can be attained.[37] Relative economic comparison of laser machining with other machining processes is made in Table 2.

Different types of lasers such as CO_2, Nd:YAG and Excimer lasers are used for machining of structural ceramics with each type of laser having its own wavelength of absorption and machining applications. CO_2 lasers are molecular lasers (subgroup of gas lasers) that use gas molecules (combination of carbon dioxide, nitrogen and helium) as the lasing medium, whereby the excitation of the carbon dioxide is achieved by increasing the vibrational energy of the molecule. The actual pumping takes place by an AC or DC electrical discharge and this laser emits light at a wavelength of 10.6 μm in the far infrared region of the electromagnetic spectrum. CO_2 lasers are widely used in industry for applications in laser machining, heat treatment and welding.[36]

On the other hand, Nd:YAG lasers are solid state lasers that use dopants (Neodinium (Nd^{3+})) dispersed in a crystalline matrix (complex crystal of Yttrium–Aluminum–Garnet (YAG) with chemical composition $Y_3Al_5O_{12}$) to generate laser light. Excitation is attained by krypton or xenon flash lamps and an output wavelength of 1.06 μm in the near-infrared region of the spectrum can be obtained. Nd:YAG fibre lasers are used in applications requiring low pulse repetition rate and high pulse energies (up to 100 J/pulse) such as hole piercing and deep keyhole welding applications.[36]

Excimer lasers are an increasingly popular type of gas lasers made up of a compound of two identical species that exist only in an excited state. Commonly used excimer complexes include argon fluoride (ArF), krypton fluoride (KrF), xenon fluoride (XeF) and xenon chloride (XeCl) with the output wavelengths varying from 0.193 to 0.351 μm in the ultraviolet to near-ultraviolet spectra. These compounds can be formed by inducing the noble gas (Ar, Kr, or Xe) of the compound into an excited state with an electron beam, an electrical discharge or a combination of the two. Excimer lasers are used for machining solid polymer workpieces, removing metal films from polymer substrates, micromachining ceramics and semi-conductors, and marking thermally sensitive materials.[36]

The different types of lasers can be operated in either the continuous wave, CW or the pulsed mode, PM (nano, pico and femto second lasers). In CW lasers, continuous pumping of the laser emits incessant light, while in a pulsed laser, there is a laser power-off period between two successive pulses.[39] Pulsed lasers are preferred for machining ceramics as the processing parameters can be more effectively controlled compared to continuous wave mode.[40] The next section looks at the important physical processes that assist in laser machining of ceramic and discusses the different types of laser machining.

Table 2
Relative economic comparisons of different machining processes[38].

Machining process	Parameter influencing economy				
	Capital investment	Toolings/fixtures	Power requirements	Removal efficiency	Tool wear
Conventional machining	Low	Low	Low	Very low	Low
Ultrasonic machining	Low	Low	Low	High	Medium
Electrochemical machining	Very high	Medium	Medium	Low	Very low
Chemical machining	Medium	Low	High	Medium	Very low
Electrical-discharge machining	Medium	High	Low	High	High
Plasma arc machining	Very low	Low	Very low	Very low	Very low
Laser machining	Medium	Low	Very low	Very high	Very low

3.1. Absorption of laser energy and multiple reflections

The physical phenomena that take place when the laser beam is incident on the ceramic surface are reflection, absorption, scattering and transmission (Fig. 4). Absorption, the vital of all the effects, is the interaction of the electromagnetic radiation with the electrons of the material and it depends on both the wavelength of the material and the spectral absorptivity characteristics of the ceramic being machined.[36,40] The absorptivity is also influenced by the orientation of the ceramic surface with respect to the beam direction and reaches a maximum value for angles of incidence above 80°.[36] For machined cavities with high aspect ratios, multiple beam reflections along the wall of cavity also affect the amount of absorbed energy.[41,42] The multiple reflections in a machined cavity are schematically represented in Fig. 5 where I_o is the incident laser energy, I_{a1}, I_{a2} and I_{a3} are the first, second and third absorptions, respectively, and I_{r1}, I_{r2} and I_{r3} are the first, second and third reflections, respectively.[43] There will be many more reflections taking place during actual ceramic machining than illustrated in Fig. 5. The phenomenon of multiple reflections has been incorporated into the machining process in several ways.[44–48] The laser beam energy Q_a absorbed by the ceramic after n reflections is:[49]

$$Q_a = Q(r)^n \quad (1)$$

where Q is incident laser beam energy, r is angle-dependent reflection coefficient of the ceramic, and n is number of multiple reflections given by:

$$n = \frac{\pi}{4\theta} \quad (2)$$

where θ is angle the cavity wall makes with normal direction. Moreover, as the thermal conductivity of structural ceramics is generally less than that of majority of metals, the energy absorption takes place faster in ceramics and 100% of incident energy is expected to be immediately absorbed by the ceramic for the machining process.[50,51] Thus the absorbed energy depends on properties of the ceramic (reflection coefficient), magnitude of incident laser energy, output wavelength of processing laser and wall angle. This energy is converted into heat and its ensuing conduction into the material establishes the temperature distribution within the material which in turn affects machining time and depth of machined cavity.

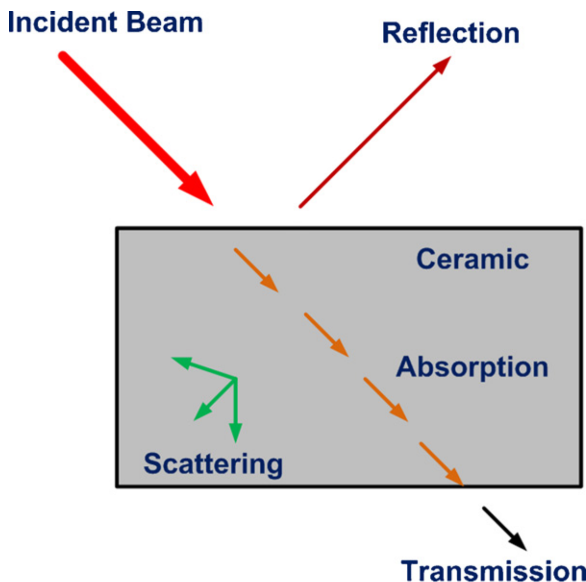

Fig. 4. Interactions of incident laser beam with ceramic.

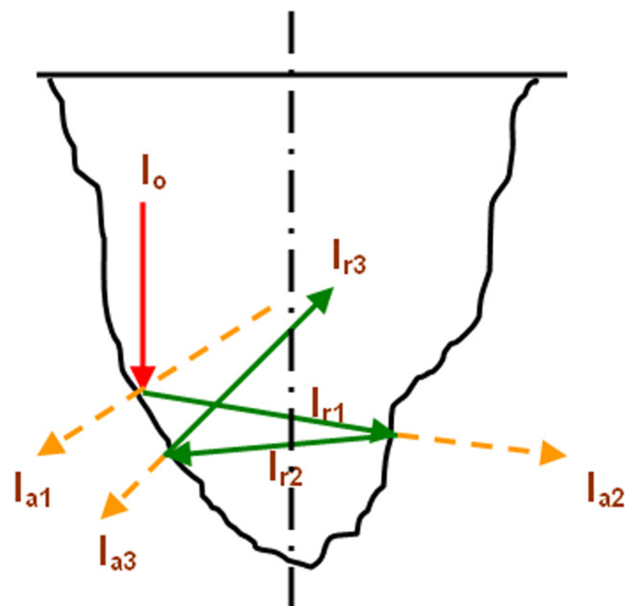

Fig. 5. Multiple reflections in a machined cavity. (After Zhao[43] with kind permission of J. Zhao's Major Professor, Dr. Vladimir V. Semak.)

3.2. Thermal effects

The excitation energy provided by the laser is rapidly converted into heat and this is followed by various heat transfer processes such as conduction into the materials, convection and radiation from the surface.[49] The conduction of heat into the ceramic is governed by Fourier's second law of heat transfer:

$$\frac{\partial T(x,y,z,t)}{\partial t} = \alpha(T)\left[\frac{\partial^2 T(x,y,z,t)}{\partial x^2} + \frac{\partial^2 T(x,y,z,t)}{\partial y^2} + \frac{\partial^2 T(x,y,z,t)}{\partial z^2}\right] \quad (3)$$

where T is temperature field, t is time and x, y and z are spatial directions. The term $\alpha(T)$ is temperature dependent thermal diffusivity of the material which is given by $k(T)/\rho C_p(T)$, where ρ is density of ceramic, $C_p(T)$ and $k(t)$ are temperature dependent specific heat and thermal conductivity of the ceramic, respectively. The balance between the absorbed laser energy at the surface and the radiation losses is given by:

$$-k(T)\left(\frac{\partial T(x,y,0,t)}{\partial x} + \frac{\partial T(x,y,0,t)}{\partial y} + \frac{\partial T(x,y,0,t)}{\partial z}\right) = \frac{\delta Q_a}{A} - \varepsilon\sigma(T(x,y,0,t)^4 - T_o{}^4) \quad (4)$$

$$\delta = 1 \quad \text{if} \quad 0 \le t \le t_p$$

$$\delta = 0 \quad \text{if} \quad t > t_p$$

where Q_a is absorbed laser power (predicted by considering multiple reflections and material properties), ε is emissivity for thermal radiation, T_o is ambient temperature, t_p is ON-time for laser, σ is Stefan–Boltzmann constant (5.67×10^{-8} W/m^2 K^4) and A is cross-sectional area of the beam. The term δ takes a value of 1 when time, t is less than laser ON-time, t_p and it is 0 when time, t exceeds laser ON-time. Thus the value of δ depends on time, t and ensures that the energy is input to the system only when the laser is ON and cuts off the energy supply when the laser is switched off. The convection taking place at the bottom

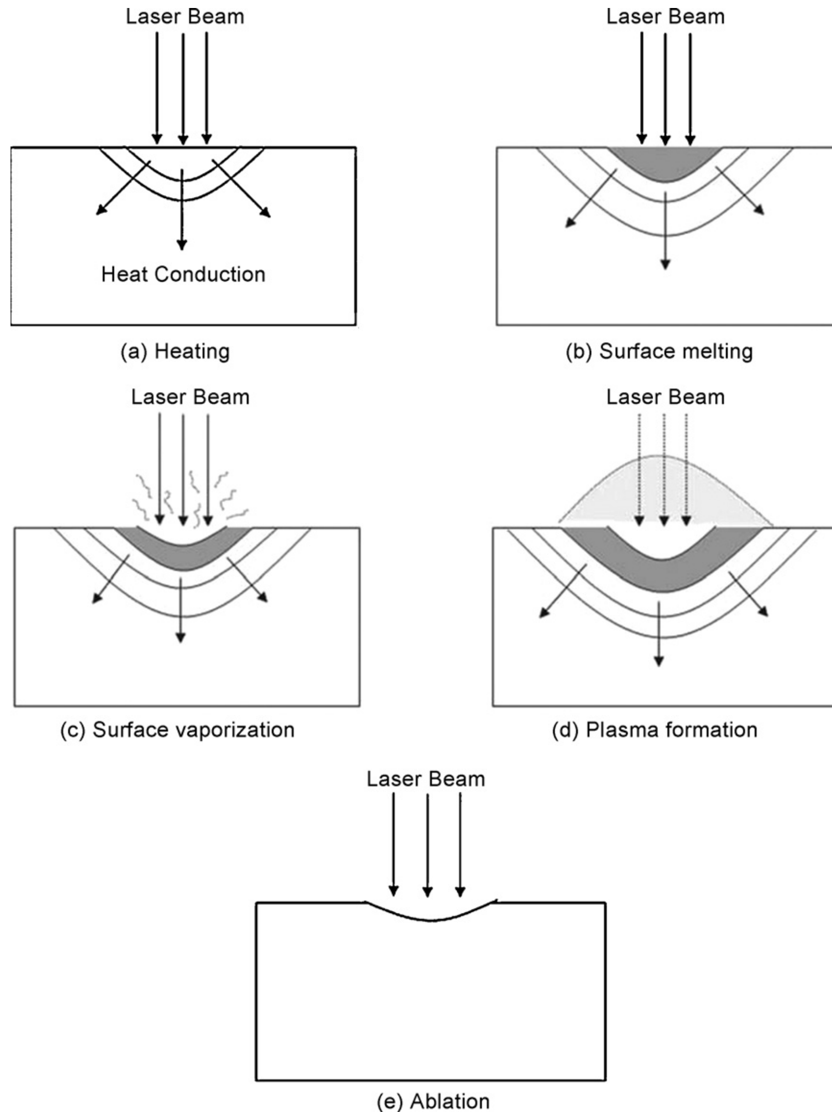

Fig. 6. Various physical phenomena during laser–ceramic interaction. (After Dahotre and Harimkar[49] with kind permission of Springer Science + Business Media.)

surface of the sample is:

$$-k(T)\left(\frac{\partial T(x,y,L,t)}{\partial x}+\frac{\partial T(x,y,L,t)}{\partial y}+\frac{\partial T(x,y,L,t)}{\partial z}\right) = h(T(x,y,L,t)-T_o), \quad (5)$$

where L is thickness of the sample being processed, h is temperature dependent heat transfer coefficient and T_o is ambient temperature. The temperature distribution within the material as a result of these heat transfer processes depends on the thermo-physical properties of the material (density, emissivity, thermal conductivity, specific heat, thermal diffusivity), dimensions of sample (thickness) and laser processing parameters (absorbed energy, beam cross-sectional area). The magnitude of temperature rise due to heating governs the different physical effects in the material such as melting, sublimation, vaporization, dissociation, plasma formation and ablation responsible for material removal/machining as discussed next (Fig. 6).[49,52,53]

3.2.1. Melting and sublimation

At high laser power densities ($I_o > 10^5$ W/cm^2), the surface temperature of the ceramic T (predicted using Eqs. (1)–(5)) may reach the melting point T_m and material removal takes place by melting as considered by Salonitis et al.[54] As indicated in Fig. 7a, the surface temperature increases with increasing irradiation time, reaches maximum temperature T_{max} at laser ON-time t_p and then decreases.[49]

The temperatures reached and the corresponding irradiation times are: $T_1 < T_m$ at time $t_1 < t_p$, T_m at time t_2, T_{max} at time t_p, T_m at time $t_3 > t_p$, and finally T_1 at time $t_4 > t_p$. The corresponding temperature profiles in the depth of the material for various times during laser irradiation are presented in Fig. 7b. The solid–liquid interface can be predicted by tracking the melting point in temperature versus depth (z) plots (Fig. 7b). For example, it can be seen from Fig. 7b that at time t_p, the position of the solid–liquid interface (melt depth) corresponds to z_{max}. Before initialization of surface evaporation, maximum melt depth increases with laser power density I (power per unit area) at constant pulse time (Fig. 8a) while at a constant laser power density, maximum depth of melting increases with increasing pulse time (Fig. 8b). Prediction of melt depth using temperature profiles obtained from Eqs. (1)–(5) assists in determining depth of machined cavity in those ceramics in which material removal takes place entirely or in part by melting.[49]

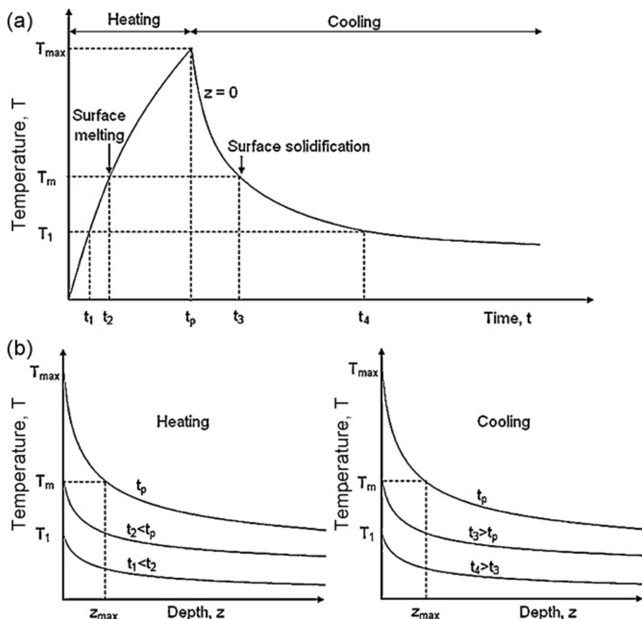

Fig. 7. Calculation of temporal evolution of melt depth (a) surface temperature as a function of time (b) temperature as a function of depth below the surface during heating and cooling. (After Dahotre and Harimkar[49] with kind permission of Springer Science + Business Media.)

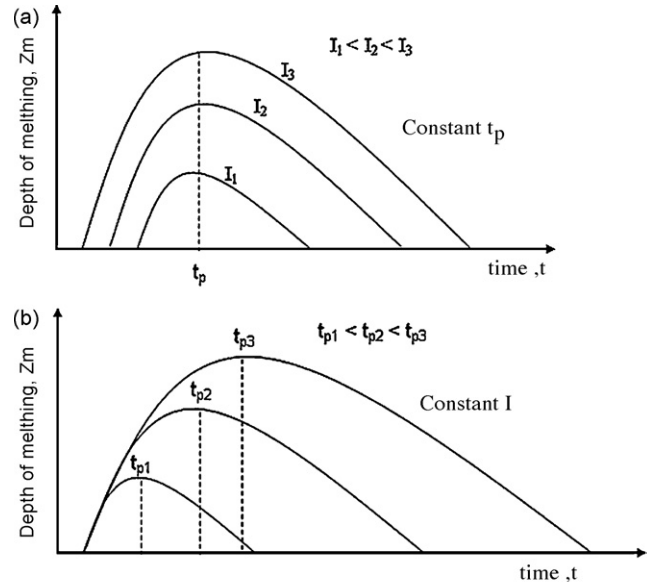

Fig. 8. Variation of melt depth during laser irradiation (a) effect of laser power density at constant pulse time (b) effect of laser pulse time at constant laser power density. (After Dahotre and Harimkar[49] with kind permission of Springer Science + Business Media.)

Some structural ceramics like Si_3N_4 do not melt but sublime, emitting N_2 and depositing a recast layer of silicon on the machined surface.[2] Attempts have been made to machine Si_3N_4 in water by Q-switched YAG lasers that can generate high peak powers (above 50 kW) from very short duration pulses (∼100 ns) at high frequency (∼10 kHz). As seen in Fig. 9, by machining

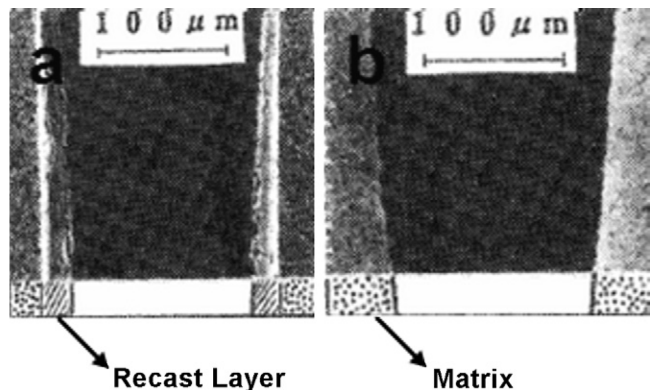

Fig. 9. Cross-section of Si_3N_4 ceramic machined in (a) air and (b) water. (After Morita et al.[55] with permission. Copyright American Institute of Physics.)

Si_3N_4 in air, a recast layer about 20 μm thick is formed and microcracks are spread within this layer. In contrast, by processing in water, no recast layers and cracks were observed. As YAG lasers retain high transmittance through water, removal of material (Si_3N_4) was possible without the formation of recast layer or micro-cracks.[55,56] The water also solidified the Si vapor and flushed away the micro-particles, thus preventing the vapor from reaching the saturation level.

3.2.2. Vaporization and dissociation

As the surface temperature of ceramic reaches the boiling point, further increase in laser power density or pulse time removes the material by evaporation instead of melting. After vaporization starts at the material surface, the liquid–vapor interface moves further inside the material with supply of laser energy and material is removed by evaporation from the surface above the liquid–vapor interface.[49] The velocity of liquid–vapor interface, $V_{\text{evaporation}}$ and the corresponding vaporization depth, $d_{\text{evaporation}}$ are given by:[52]

$$V_{\text{evaporation}} = \frac{Q_a}{\rho(cT_b + L_v)} \quad (6)$$

$$d_{\text{evaporation}} = \frac{Q_a t_p}{\rho(cT_b + L_v)} \quad (7)$$

where Q_a is absorbed laser energy (Eq. (1)), ρ is density of the ceramic, c is the speed of light, T_b is the boiling point of the ceramic, L_v is the latent heat of vaporization and t_p is ON-time for laser (time for which the ceramic surface is exposed to incident laser energy). Several works in the past have considered material removal only through this direct evaporation mechanism.[57–61] In such cases, the depth of evaporation (Eq. (7)) corresponding to depth of machined cavity depends on the laser conditions (processing time and absorbed laser energy) and material properties such as density, latent heat of vaporization, and boiling point.

Certain ceramics such as SiC, MgO directly dissociate/decompose into several stoichiometric and/or non-stoichiometric species depending on the thermodynamic conditions prevailing during laser machining. Alumina, on the other hand is stable up to 2327 K after which it melts and forms liquid. This liquid remains stable from 2327 to 3500 K and sub-oxides of aluminum, aluminum metal vapor and gaseous oxygen are formed due to the dissociation above 3250 K. The dissociation reaction forms different species that are expelled/removed during machining process and dissociation energy losses also affect the input laser energy and thus the temperature distribution, dimensions of machined cavity and machining time.[62–66]

The evolving vapor from the surface applies recoil pressure (p_{recoil})[67,68] on the surface given by:[69]

$$\frac{A p_{\text{recoil}}}{Q_a} = \frac{1.69}{\sqrt{L_v}} \left(\frac{b}{1 + 2.2b^2} \right) \quad (8)$$

where $b^2 = kT_s/m_v L_v$, T_s is surface temperature, k is the Boltzmann constant (1.38065×10^{-23} J/K), m_v is the mass of vapor molecule, A is beam cross-sectional area, Q_a is absorbed laser energy, and L_v is the latent heat of vaporization. The absorbed laser energy (Eqs. (1) and (2)) and the associated surface temperatures predicted using Eqs. (3)–(5) affect the recoil pressure which plays a vital role in material removal in molten state during machining of some ceramics such as SiC, Al_2O_3 and Si_3N_4.

Table 3
Physical phenomena governing machining in some structural ceramics (√ – phenomena present; × – phenomena not present)[64].

Material	Physical process		
	Melting	Dissociation	Evaporation
Silicon carbide (SiC)	√	√	√
Alumina (Al_2O_3)	√	√	√
Silicon nitride (Si_3N_4)	√	√	√
Magnesia (MgO)	×	√	√

The total enthalpy required for laser-induced vaporization being greater than that required for melting, the energy required for laser machining by melting is much less than the energy required for machining by vaporization.[26] It was reported by Samant and Dahotre[62–66] that a combination of the different physical phenomena mentioned above was responsible for machining rather than any single predominant process. The machining mechanisms depending on the nature of some of the commonly used structural ceramics are represented in Table 3 and will be discussed elaborately in the later part of this study.

3.2.3. Plasma formation

When the laser energy density surpasses a certain threshold limit, the material immediately vaporizes, gets ionized and forms plasma having temperatures as high as 50,000 °C and pressures up to 500 MPa.[70] The degree of ionization (ξ) depends on the surface temperatures (predicted from Eqs. (1)–(5)) and is given by the Saha equation:[26]

$$\frac{\xi^2}{1-\xi} = \frac{2g_i}{g_a N_g} \left(\frac{2\pi m_v k T_s}{h^2} \right)^{3/2} \exp\left(-\frac{E_i}{kT_s} \right) \quad (9)$$

where $\xi = N_e/N_g$ and $N_g = N_e + N_a$. N_e and N_a are the number densities of electrons and atoms/molecules respectively, g_i and g_a are the degeneracy of states for ions and atoms/molecules, E_i is the ionization energy, m_v is the mass of vapor molecule, k is the Boltzmann constant (1.38065×10^{-23} J/K), T_s is surface temperature, and h is Planck's constant (6.626×10^{-34} m^2 kg/s). The plasma plume forms a shield over the machining area and reduces the energy available to the work piece when the surface temperature exceeds a certain threshold value. Aerosols formed due to the condensation of ionized material vapor stick to the surface and reduces the efficiency of machined components for applications dominated by wear or tear load. Hence the degree of ionization is an important parameter which gives an indication whether plasma will be formed during the machining process and accordingly, necessary efforts to overcome the harmful effects of plasma could be undertaken. A special gas nozzle designed by Tönshoff et al.[71] (Fig. 10) prevents the deposition of aerosols and this technique has been successfully applied to machine SiC ceramic surfaces without any debris.[70] The additional gas stream obtained by combining a process gas

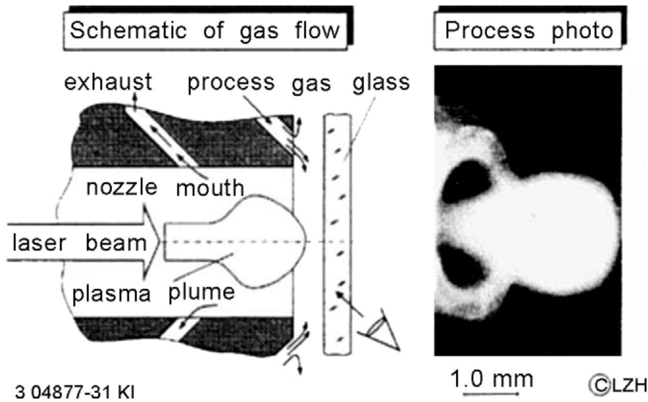

Fig. 10. Formation of plasma plume and its suction by gas nozzle. (After Tönshoff and Kappel[70] with permission. Copyright Elsevier.)

stream and an exhaust stream transports the vaporized material and avoids radial distribution of the plasma.

A technique developed at the Integrated Manufacturing Technologies Institute (IMTI), National Research Council Canada (NRC) minimizes the harmful effects of the plasma and provides a precise control over the material removal rate and surface finish. This technique controls the pulse duration and energy per pulse such that majority of the energy in a pulse instantaneously vaporizes a given quantity of the material from the surface. Continuous application of laser pulses ensures that each successive spot is adequately displaced to reduce the plasma absorption effects. Furthermore, short duration pulses reduce the recast layer thickness, eliminate micro-cracks and the material removed per pulse increases with increasing energy density while machining TiN/Si_3N_4 and SiC/Si_3N_4 materials (Fig. 11).[72]

3.2.4. Ablation

When the material is exposed to sufficiently large incident laser energy, the temperature of the surface exceeds the boiling point of the material causing rapid vaporization and subsequent material removal by the process referred to as thermal ablation.[26] Ablation takes place when laser energy exceeds the characteristic threshold laser energy which represents the minimum energy required to remove material by ablation. The complex laser–material interaction during ablation depends on the interaction between the photo-thermal (vibrational heating) and photo-chemical (bond breaking) processes. Above ablation threshold energy, material removal is facilitated by bond breaking, whereas thermal effects take place below ablation threshold energy. Absorption properties of the ceramic and incident laser parameters determine the location at which the absorbed energy reaches the ablation threshold, thus determining the depth of ablation, d_{ablation} given by:[49]

$$d_{\text{ablation}} = \frac{1}{\mu_a} \ln\left(\frac{Q_a}{Q_{\text{th}}}\right) \tag{10}$$

where μ_a is absorption coefficient of ceramic and Q_{th} is threshold laser energy. The ablation rates and associated machined depths are governed by laser energy Q_a (predicted from Eq. (1)), pulse duration, number of pulses and pulse repetition rate. Yttrium stabilized Si–Al–O–N (Y-sialon) was irradiated by an Kr-F-excimer laser at a fluence of 850 mJ/cm^2, pulse repetition rate varying from 2 to 20 Hz and by applying different number of pulses.[73] The material removal in Y-sialon under the above processing conditions was by ablation. The variation of ablation depth and a Y-sialon sample ablated by laser irradiation is presented in Fig. 12a and b, respectively.

The above described physical processes can be incorporated into a computational model and used to predict the maximum temperatures attained during machining in addition to several

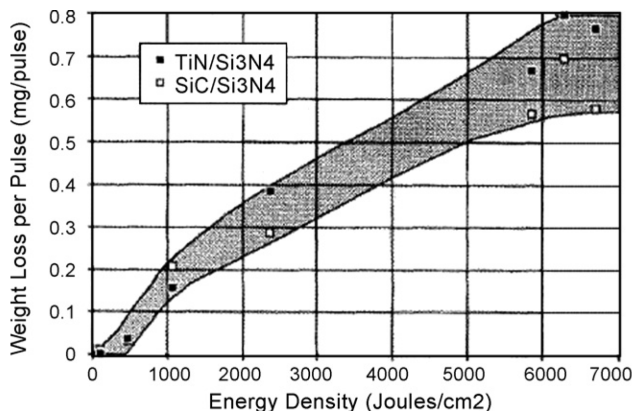

Fig. 11. Variation of material removal rate with energy density. (After Islam[72] with kind permission of Springer Science + Business Media.)

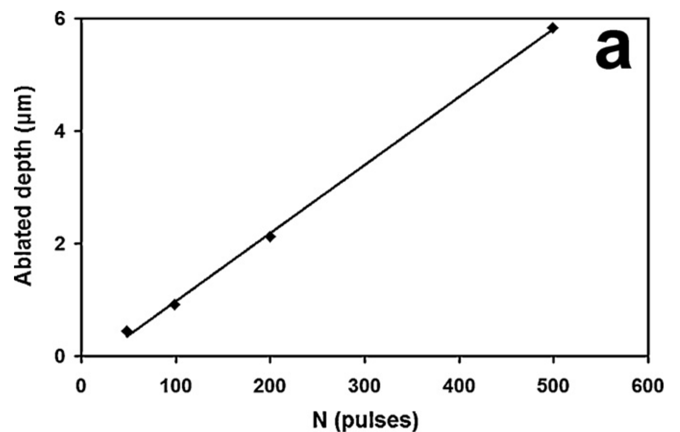

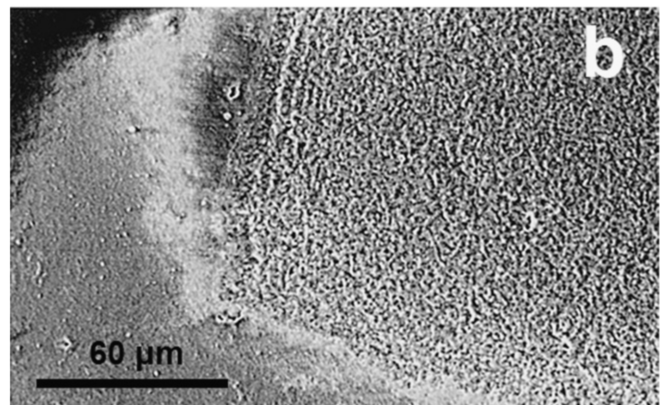

Fig. 12. (a) Ablation profile of Y-sialon under irradiation (b) ablated region in Y-sialon. (After Laude et al.[73] with permission. Copyright Elsevier.)

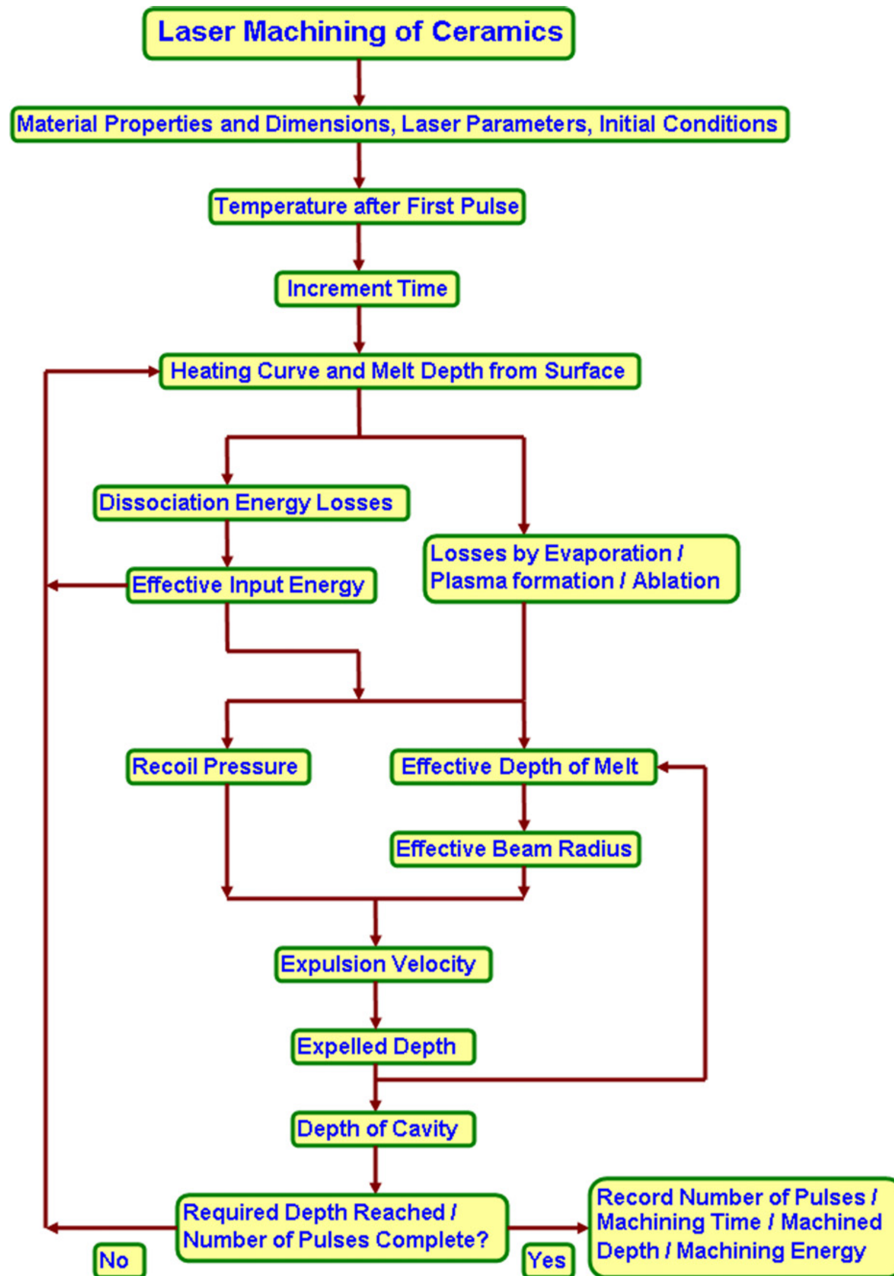

Fig. 13. Stepwise procedure for prediction of machining parameters.

other parameters such as machining time, number of pulses, dimensions of machined cavity and machining energy. In light of this, an ab initio physical model was developed by Samant and Dahotre and used for predicting depth of machined cavity when a certain number of pulses was applied to Si_3N_4[62] and also for advance prediction of number of pulses and energy necessary for machining SiC ceramic.[66] The model was also applied to determine the number of pulses and corresponding time required for machining a certain depth in Al_2O_3[63] and MgO.[65] A general flow chart for predicting the desired machining parameter based on such computational model using the process parameters and material properties is represented in Fig. 13. The nature of the structural ceramic will govern the physical phenomena that can be incorporated into the mathematical model.

3.3. Types of machining

Based on the kinematics of the front in the area where material removal takes place, laser machining is classified into one-, two-, and three-dimensional machining. The laser beam is considered as a one-dimensional line source with line thickness given by the diameter for circular and the major axis for elliptical beam cross-sections. Laser drilling (one-dimensional) machining (Fig. 14a) can be achieved by keeping the ceramic workpiece as well as the laser beam stationary while the motion of the laser beam or the ceramic in only one direction leads to cutting (two-dimensional machining) (Fig. 14b) in the ceramic. Motion of one or more laser beams or the workpiece in more than one direction leads to

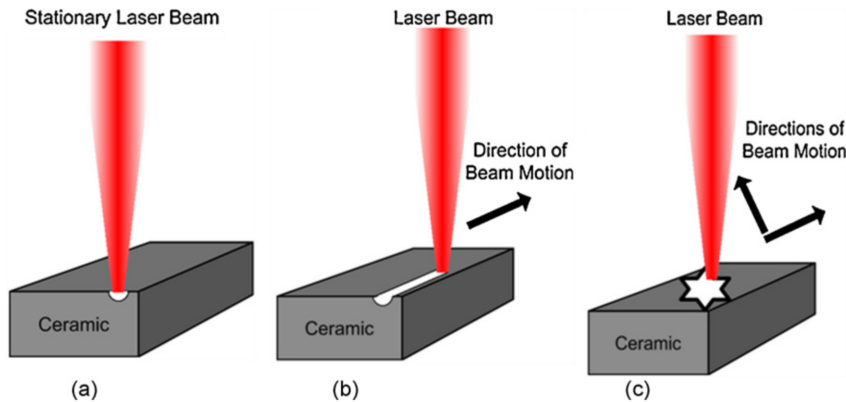

Fig. 14. Schematic of basic laser machining processes (a) laser drilling (one-dimensional machining), (b) laser cutting (two-dimensional machining), (c) engraving a star by laser beam (three-dimensional machining).

three-dimensional machining and complex geometries can be machined (Fig. 14c).

3.3.1. One-dimensional laser machining

Drilling is a one-dimensional laser machining process where the laser beam is fixed relative to the workpiece. The material removal rate is governed by the velocity of the erosion front in the direction of the laser beam. The hole taper is a measure of the dimensional accuracy for laser drilling and it can be minimized to an insignificant order of appearance by using a lens of long focal length with longer focal waist. A schematic of the laser drilling process and a hole drilled in SiC with associated microstructural features is presented in Figs. 15 and 16, respectively.[74] The drilling in SiC was carried out using a pulsed CO_2 laser ($\lambda = 10.6\ \mu m$) with a pulse duration of 2 ms, a power of 0.5 kW and the lens had a focal length of 31.8 mm.

3.3.2. Two-dimensional laser machining

In two-dimensional laser machining (cutting), the laser beam is in relative motion with respect to the workpiece (Fig. 17). A cutting front is formed when the laser beam melts/vaporizes the material throughout the thickness or the depth. In addition to removal of the molten material, the pressurized gas jet

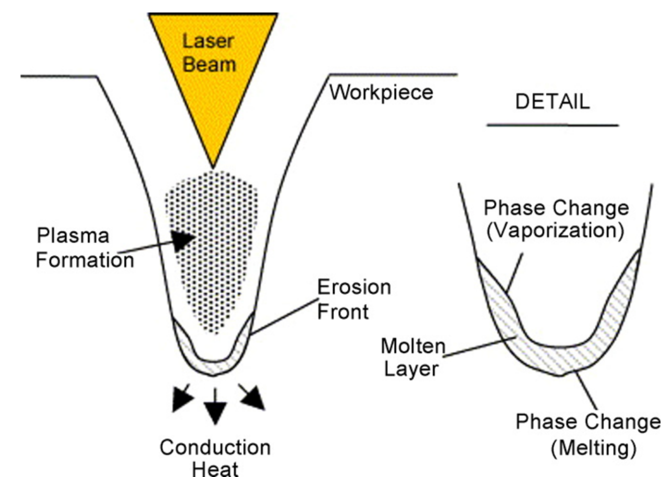

Fig. 15. Laser drilling process schematic. (After Chryssolouris[36] with kind permission of Springer Science + Business Media.)

also assists in enhanced material removal by chemical reactions such as oxidation. Cutting of the material then proceeds by the motion of the cutting front across the surface of the material.[75] The four main techniques associated with laser cutting are evaporative laser cutting, fusion cutting, reactive fusion cutting and controlled fracture technique. The selection of the machining method depends on the thermo-physical properties of the material, workpiece thickness and type of laser used.

Brittle ceramics such as alumina are mostly machined by the controlled fracture technique where the incident laser energy generates localized mechanical stresses that cause the material to separate by crack extension with controllable fracture growth. The energy requirement is less compared to conventional evaporative laser cutting as the material removal is by crack propagation. The experimental setup in Fig. 18a consists of a personal computer, a CO_2 laser, a Nd:YAG laser and a XYZ positioning table. The focused Nd:YAG laser having a focal plane on the surface of the substrate and the beam orthogonal to the surface is used to scribe a groove on the ceramic surface. The defocused CO_2 laser inclined to the Nd:YAG laser beam induces localized thermal stresses in the substrate. Both the laser beams are applied simultaneously on the ceramic surface in a continuous mode of operation. The stress concentration at the groove tip assists in extending the crack through the substrate followed by controlled separation along the moving path of the laser beam.[76] The four distinct regions: evaporation, columnar grain, intergranular fracture, and transgranular fracture regions of the alumina ceramic cut by controlled fracture technique is presented in Fig. 18b.

3.3.3. Three-dimensional laser machining

Two or more laser beams are used for three-dimensional machining and each beam forms a surface with relative motion with the workpiece (Fig. 19). The erosion front for each surface is located at the leading edge of each laser beam. When the surfaces intersect, the three-dimensional volume bounded by the surfaces is removed and machining takes place. Laser turning and milling are commonly used three-dimensional laser machining techniques useful for machining complex geometries such as

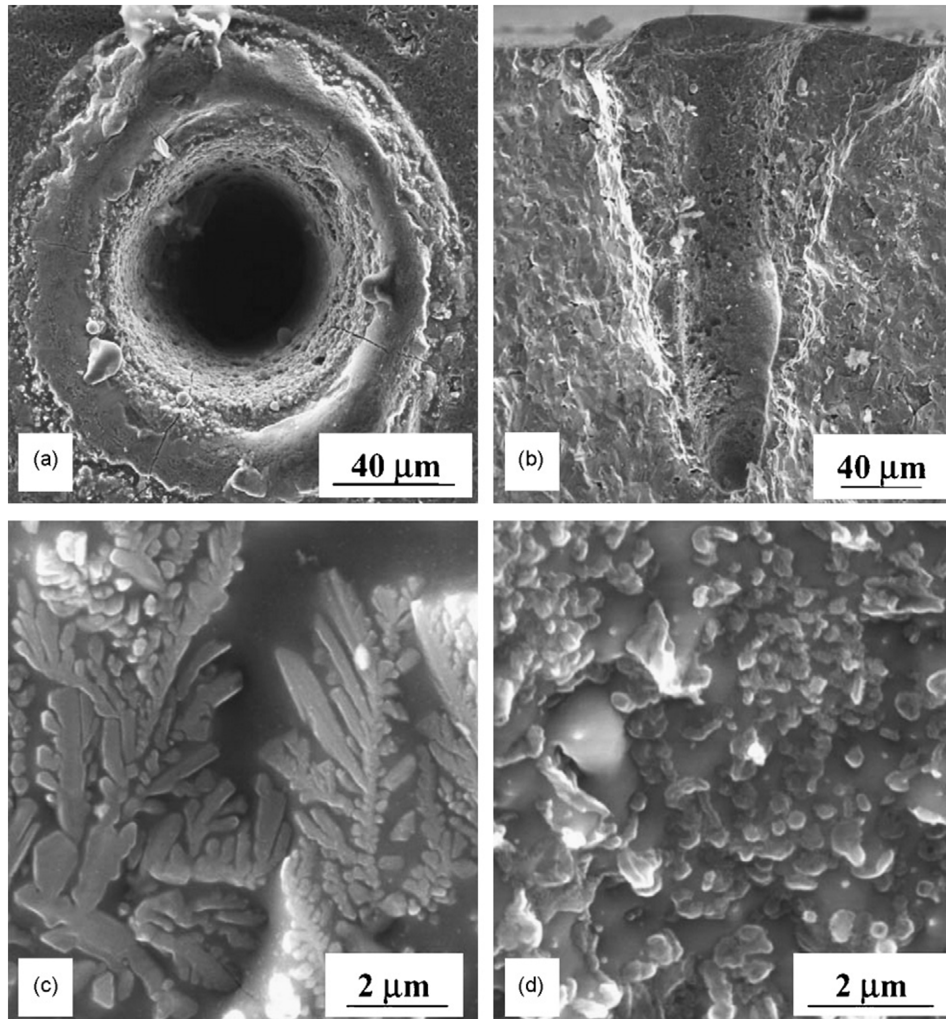

Fig. 16. Microstructural features of hole obtained in SiC (a) hole entry (b) hole section (c) silicate-like dendrite crystals obtained on debris area (d) hole inside walls. (After Sciti and Bellosi[74] with permission. Copyright Elsevier.)

slots, grooves, threads, and complex patterns in ceramic workpieces. Laser machining has been used to turn threads in Si_3N_4 ceramic (Fig. 20a)[77] and also to cut gears from SiC_ω/Al_2O_3 composite (Fig. 20b).[72]

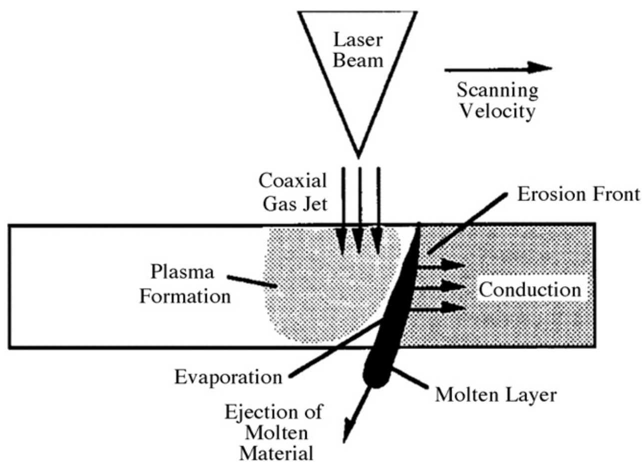

Fig. 17. Schematic of laser cutting process. (After Chryssolouris[36] with kind permission of Springer Science + Business Media.)

4. State of the art

So far it has been covered in this study that temperature dependent thermo-physical properties and laser processing conditions govern the physical phenomena that can machine ceramics in one, two or three dimensions. Even though a few structural ceramics have been briefly mentioned earlier only to explain key concepts of laser machining, this section presents the detailed state of the art in machining by lasers of some commonly used structural ceramics such as Al_2O_3, Si_3N_4, SiC, AlN, ZrO_2, and MgO.

4.1. Alumina

Besides the applications mentioned earlier, alumina is also used as a substrate in hybrid circuits as it possesses excellent dielectric strength, thermal stability and conductivity.[78] CO_2 lasers have been adapted for drilling holes in thin alumina plates used as substrates for thin-film circuits in electronic switching systems. Hole diameters varying from 0.125 to 0.3 mm were drilled by changing the lenses and the pulse duration.[79] Laser

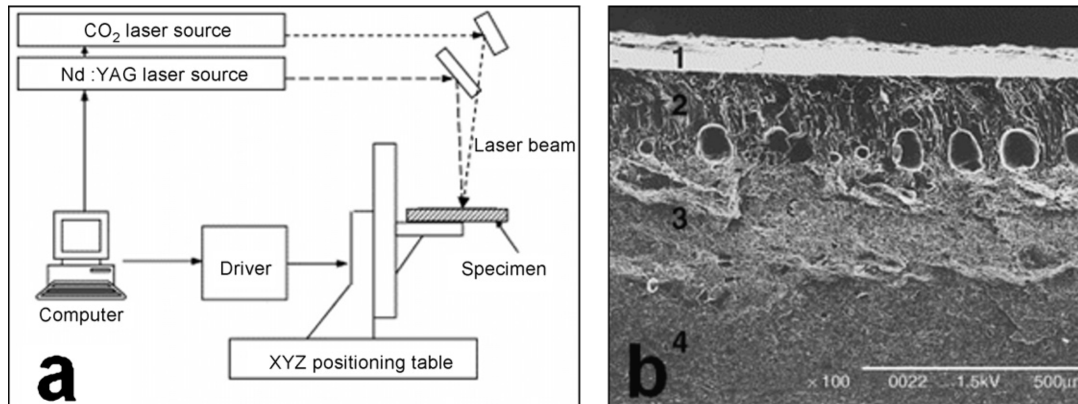

Fig. 18. (a) Configuration of laser cutting using controlled fracture technique. (b) Fracture surface of alumina substrate. (After Tsai and Chen[76] with permission. Copyright Elsevier.)

scribing (drilling a series of blind holes in a line) was carried out by Saifi and Borutta[80] with a pulsed CO_2 laser for separating individual thin-film circuits on a large substrate. It was observed that for shorter pulse length, the heat-affected zone was small with a corresponding rapid temperature drop. On the other hand, the development of microcracks in the scribed region reduced the flexural strength of the scribed substrates.

Holes of variable depths were drilled in dense alumina ceramic using a pulsed Nd:YAG laser (1064 nm wavelength) by applying different number of pulses at a pulse energy of 4 J, repetition rate of 20 Hz and a pulse width of 0.5 ms (Fig. 21). Laser fluences of 442, 884, 1768 and 2652 J/cm^2 were required for drilling depths of 0.26, 0.56, 3.23, and 4.0 mm.[63] As mentioned earlier, alumina liquid is formed at 2327 K which is stable till 3500 K. At temperatures above 3250 K, dissociation of the ceramic yields different species such as AlO(g), Al(l), Al(g), Al_2O(g) and AlO_2(g).[81] At temperatures above 5000 K, dissociation is complete and aluminum vapor and atomic oxygen are formed. Recoil pressure provoked expulsion of the liquid phase formed due to melting between 2327 and 3500 K and the dissociation process above 3250 K (most likely by reaction in Eq. (11)) is responsible for laser machining in alumina.

$$Al_2O_3 = 2Al(l) + \frac{3}{2}O_2(g) \tag{11}$$

There was also some material loss at the surface by evaporation and the machining in alumina was a combined effect of melt expulsion, dissociation and evaporation.[63]

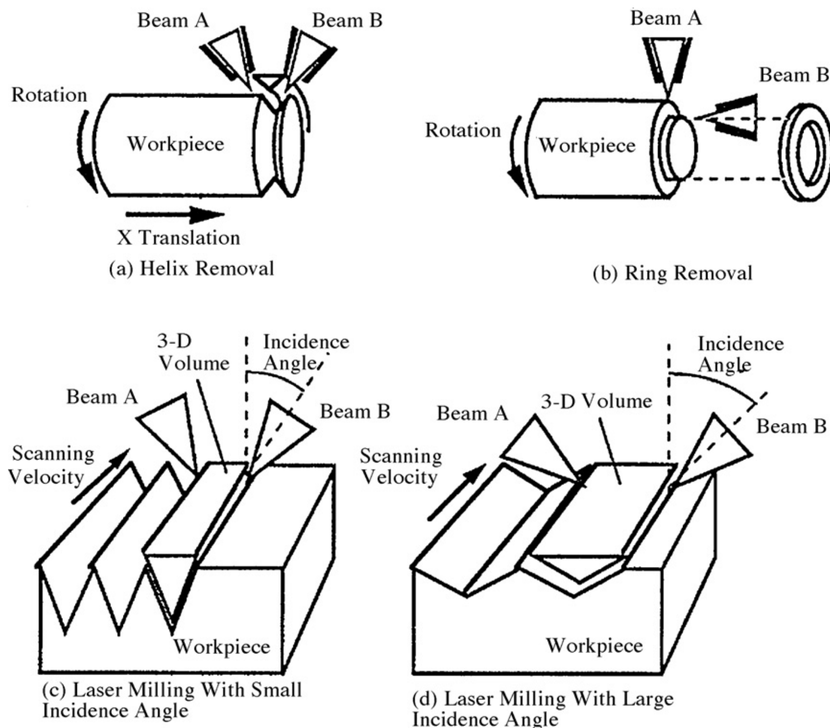

Fig. 19. Three-dimensional laser machining. (After Chryssolouris[36] with kind permission of Springer Science + Business Media.)

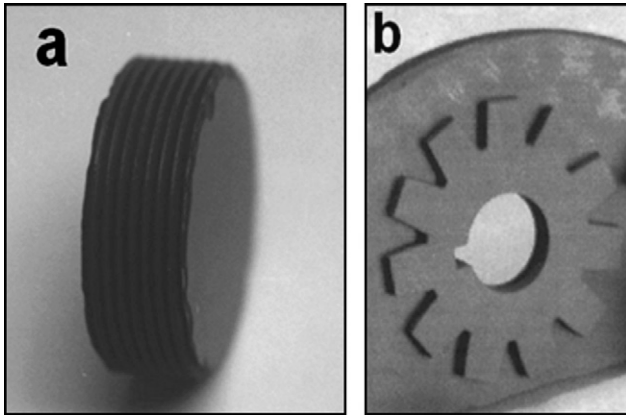

Fig. 20. (a) Turning of threads in Si_3N_4. (After Liu et al.[77] with permission. Copyright Elsevier.) (b) A gear shape cut in $SiC_{\omega}18/Al_2O_3$ composite. (After Islam[72] with kind permission of Springer Science + Business Media.)

The threshold energy density (the minimum energy density required for material removal) for drilling gold-coated alumina by ruby lasers (400 J/cm^2) was less than the energy density for drilling uncoated alumina (750–1000 J/cm^2). This drop in energy density could be attributed to the relatively high thermal conductivity of gold.[82] Drilling of 0.25 mm diameter holes in 0.1 mm thick alumina workpiece was performed by Coherent, Inc. at a machining speed of 0.1 s/hole using a pulsed CO_2 laser at a pulse frequency of 500 Hz and pulse duration of 200 ms.[83] Chryssolouris and Bredt[84] drilled blind holes (depths varying from 0.02 to 1 cm) using a 1.2 kW CW CO_2 laser with energy densities ranging from 2 to 500 kJ/cm^2. CO_2 and Nd:YAG lasers with power densities between 10^6 and 10^8 W/cm^2 were used to drill holes in alumina upto 0.25 mm diameter and it was found that the holes drilled by CO_2 laser showed a noticeable taper compared to the holes made by Nd:YAG laser.[85]

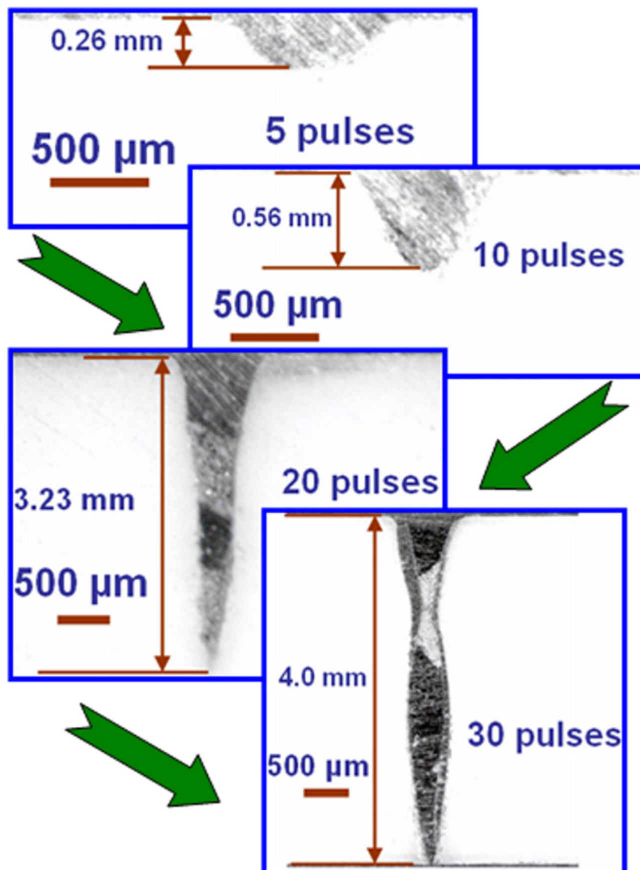

Fig. 21. Drilling in dense alumina ceramic. (After Samant and Dahotre[63]).

Common defects associated with laser drilling (Microcracks and spatter[86–89]) were prevented by a drilling technique based on gelcasting.[90] For gelcasting, the ceramic slurry made by dispersing the powders in a pre-mixed monomer solution is cast in a mold of desired shape. After addition of a suitable initiator, the entire system is polymerized in situ and green bodies with improved mechanical properties are produced. As the green body has relatively loose structures compared with sintered ceramics, spatter-free holes with more uniform shapes and without microcracks can be drilled (Fig. 22).

A computer controlled Nd:YAG laser was used to obtain good quality kerfs and cuts without cracks in alumina substrates for embedded MCM-Ds (Multi Chip Modules, deposited) and water-cooled heat sinks for single chips, multi chip modules or laser diodes. A laser energy of 1.7 J, pulse duration of 0.4 ms, pulse frequency of 250 Hz, nitrogen as process gas and a feed rate of 150 mm/min were used for machining these substrates.[91] Alumina has also been machined with a KrF excimer laser with laser fluence (1.8 and 7.5 J/cm^2), pulse duration (25 ns), number of pulses (1–500), frequency (1–120 Hz), and the corresponding microstructural changes were examined.[92] At low fluence (1.8 J/cm^2), the melting/resolidification produced scales on the surface while at high fluence (7.5 J/cm^2), there were no continuous scales as the material was removed by vaporization. The depth of material removed was directly proportional to the number of pulses.[63,92] However, this laser treatment was not suitable for reducing the roughness as can be seen from Fig. 23 that the values of Ra (surface roughness) and Rt (peak-to-valley distance) varied slightly compared to the starting values. Moreover, Femtosecond near-infrared (NIR) optical pulses have been used for microstructuring alumina with improved edge quality at scanned intensities less than 50 W/cm^2.[78] The surface showed no discoloration unlike the processing done by nanosecond UV lasers at 248 nm wavelength by Sciti et al.[92]

3D Laser Carving is an emerging technique in industries for manufacturing ceramic components of complex shapes. Initially, a 3D CAD model is sliced in a particular direction to obtain profile information of the slice. The focused laser beam is then used for scanning and engraving the ceramic surface as per the profile information, producing two-dimensional layer patterns. Finally, the *Z*-axis of the table is raised to a designated height to locate the carving surface at the focal plane. This process is repeated several times until the whole model is completely sliced and the 3D graphics is engraved on the workpiece (Fig. 24).[93] Thus, alumina ceramic has been laser machined in one, two and three dimensions by using different types of lasers for several applications.

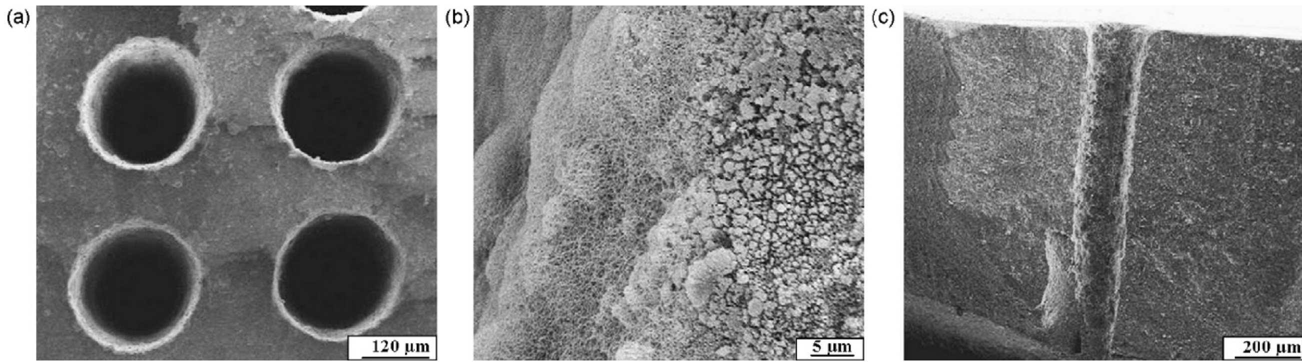

Fig. 22. Holes drilled on gelcast green body of alumina. (a) Top view, (b) hole edge, (c) cross-section of hole. (After Guo et al.[90] with permission. Copyright Elsevier.)

4.2. Silicon nitride

Silicon nitride is widely used for machining purposes in automotive, semi-conductor and aerospace industries. Cams, bearings, piston rings and rocker arms can be made by machining this ceramic.[94,95] A 0.1 mm hole drilled at the Integrated Manufacturing Technologies Institute (IMTI), National Research Council Canada (NRC) through a 6 mm thick silicon nitride cutting tool insert is presented in Fig. 25.[72] Harrysson et al. drilled holes in Si_3N_4 using CO_2 and Nd:YAG lasers. High thermal stresses produced intense cracking in CO_2 laser drilled samples while the cracking was limited only to the recast layer (about 0.02 mm) by using a Nd:YAG laser.[96] A pulsed Nd:YAG laser at a pulse energy of 4 J, pulse width of 0.5 ms and a repetition rate of 20 Hz was used for drilling holes of varying depths in Si_3N_4 by applying different number of pulses (Fig. 26).[62]

The decomposition of Si_3N_4 into N_2 gas and Si liquid (Eq. (12))[97] at the sublimation temperature of Si_3N_4 followed by the expulsion of the liquid silicon was proposed as the material removal mechanism.[98,99]

$$Si_3N_4 = 3Si(l) + 2N_2(g) \quad (12)$$

There were some evaporative losses at the surface and a combination of melting, dissociation and evaporation lead to machining in silicon nitride (Table 3).[62] In excimer laser processing by ArF, KrF and XeF excimer lasers, decomposition of Si_3N_4 into Si (gas) and nitrogen along with ionized silicon produced excellent quality of the processed ceramic without deposition of any decomposed material.[100] Shigematsu et al. machined Si_3N_4 in different atmospheres (N_2, O_2 gas and air) by a multi-mode CO_2 laser and the particles suspended in the chamber after machining were studied.[101] The infrared spectra of the gases and the suspended particles inside the chamber are presented in Fig. 27. No absorption peaks were observed in N_2 and all the liquid silicon formed by Eq. (12) above was deposited on the ceramic surface. The energy density of the CO_2 laser was insufficient to vaporize the free silicon. Machining in O_2 or air formed SiO vapor by the oxidation decomposition of Si_3N_4:

$$2Si_3N_4(s) + 3O_2 = 6SiO(g) + 4N_2(g) \quad (13)$$

The SiO vapor immediately oxidized and formed solid phase SiO_2 seen in the absorption spectrum:

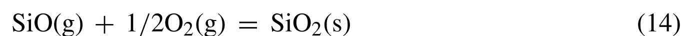

$$SiO(g) + 1/2O_2(g) = SiO_2(s) \quad (14)$$

Machining in O_2 also released NO_2 gas:

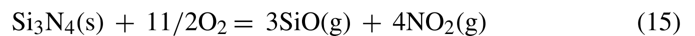

$$Si_3N_4(s) + 11/2O_2 = 3SiO(g) + 4NO_2(g) \quad (15)$$

Such an analysis of the constituents released during machining can help in the selection of an appropriate machining environment and laser machining parameters.

CO_2 laser was operated in continuous and pulsed mode for cutting Si_3N_4 and it was found that deep and narrow cuts were produced by pulsed mode as compared to continuous mode of

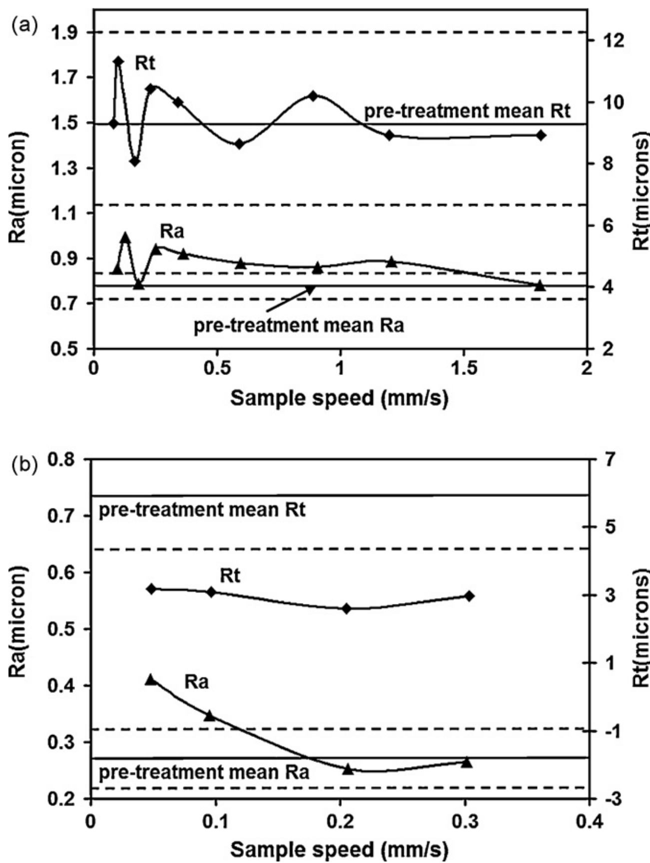

Fig. 23. Surface roughness after laser treatment for (a) raw Al_2O_3 at fluence of 1.8 J/cm^2 and (b) polished Al_2O_3 at fluence of 7.5 J/cm^2. (After Sciti et al.[92] with kind permission of Springer Science + Business Media.)

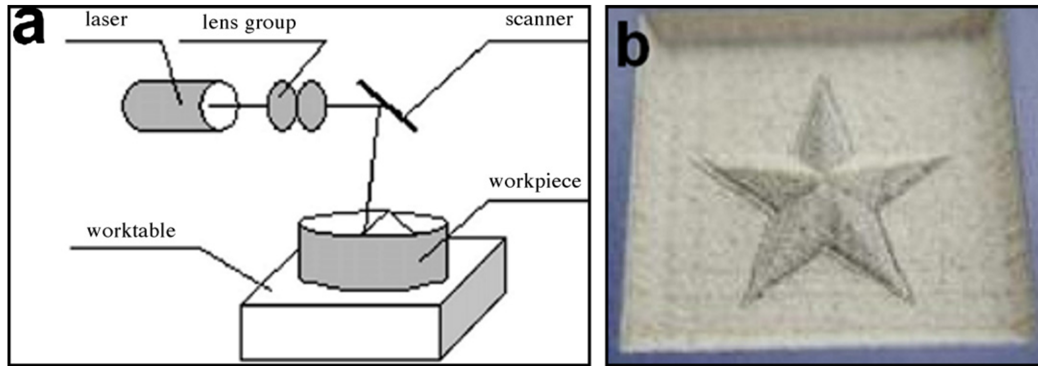

Fig. 24. 3D Laser Carving (a) schematic layout (b) 3D star in alumina ceramic. (After Wang and Zeng[93] with permission. Copyright Elsevier.)

operation. Reducing the traverse speed avoided fracture of the ceramic and it was more effective than increasing the laser power for machining thicker plates (6–8 mm).[102] Firestone et al. used a 15 kW CO_2 laser to machine silicon nitride without fracturing at 996 °C and the machining rates achieved were ten times that of conventional diamond grinding.[103] This ceramic has also been machined by Lavrinovich et al. in two regimes: with free generation where the width of the laser pulse was 4 ms and with Q-factor modulation where the pulse width was 3×10^{-7} s.[104] Q-factor modulation was able to form an oxide film on the surface when exposed to a defocused laser beam. This method also helped to minimize the residual microcracks.

Apart from the above applications of laser machining of silicon nitride, laser milling is a newly developed method of producing wide variety of complex parts from ceramics such as silicon nitride directly using the CAD data, thus making it possible to machine Si_3N_4 in one, two and three dimensions.[105]

4.3. Silicon carbide

Silicon carbide is another structural ceramic that has been widely machined by lasers for different purposes. Using a pulsed

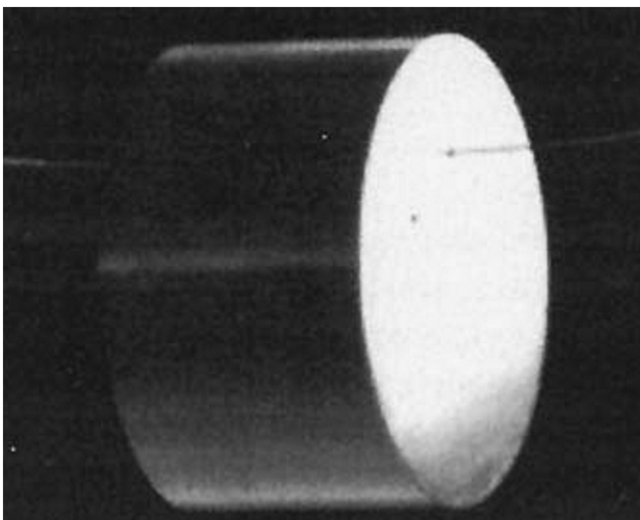

Fig. 25. A 0.1 mm diameter hole drilled in 6 mm thick Si_3N_4 cutting tool insert. Wire passing through the hole is also seen. (After Islam[72] with kind permission of Springer Science + Business Media.)

Nd:YAG laser (1064 nm wavelength) at an input energy of 6 J, pulse duration of 0.5 ms, and repetition rate of 50 Hz, a through cavity was machined in a 2 mm thick SiC plate in approximately 25 pulses while it took about 125 pulses to machine through the entire thickness of a 3 mm thick plate (Fig. 28).[66] Sciti and Bellosi used a pulsed CO_2 laser with laser powers of 0.5 and 1 kW for drilling the ceramic surface.[74] The beam was incident on the surface at an angle of 90° and three different focal lengths of 95.3, 63.5, and 31.8 mm were used for machining. The hole depth increased with the pulse duration and also the input power for a given focal length because of increase in laser light intensity. Even though the hole diameters remained constant with pulse duration, they were affected by the lens focal length that governed the size of the laser spot (Fig. 29).

Metallic silicon particles were found on the surface of the silicon carbide ceramics machined in N_2, O_2, or air.[101] CO_2 formed by the oxidization of free carbon released by the dissociation of SiC was also detected in the machining atmosphere (Eqs. (16)–(18)).[101]

$$SiC(s) = Si(l) + C(s) \tag{16}$$

$$2C(s) + O_2(g) = 2CO(g) \tag{17}$$

$$2CO(g) + O_2(g) = 2CO_2(g) \tag{18}$$

Furthermore, machining in air or O_2 and in N_2 produced SiO_2 (Eqs. (19)–(20)) and toxic cyanogen respectively (Eq. (21)).[101]

$$2SiC + O_2(g) = 2SiO(g) + 2C(s) \tag{19}$$

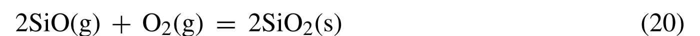
$$2SiO(g) + O_2(g) = 2SiO_2(s) \tag{20}$$

$$2C + N_2(g) = (CN)_2(g) \tag{21}$$

Looking at the released constituents can assist in choosing a suitable working atmosphere based on safety and health requirements. A 400 W Nd:YAG laser with pulse frequencies upto 200 Hz and pulse width of 250 to 1000 ms was capable of drilling holes (0.25–1.5 mm diameter) in 3–3.5 mm thick SiC plates along with other ceramics such as silicon nitride and alumina.[106] It was found that SiC required the highest pulse energy of all ceramics and corresponding holes produced had the most irregular shape.

Affolter et al. cut 5 mm thick SiC plates with a 10 kW Nd:YAG laser at a cutting speed of 40 mm/min[107] while a 15 kW

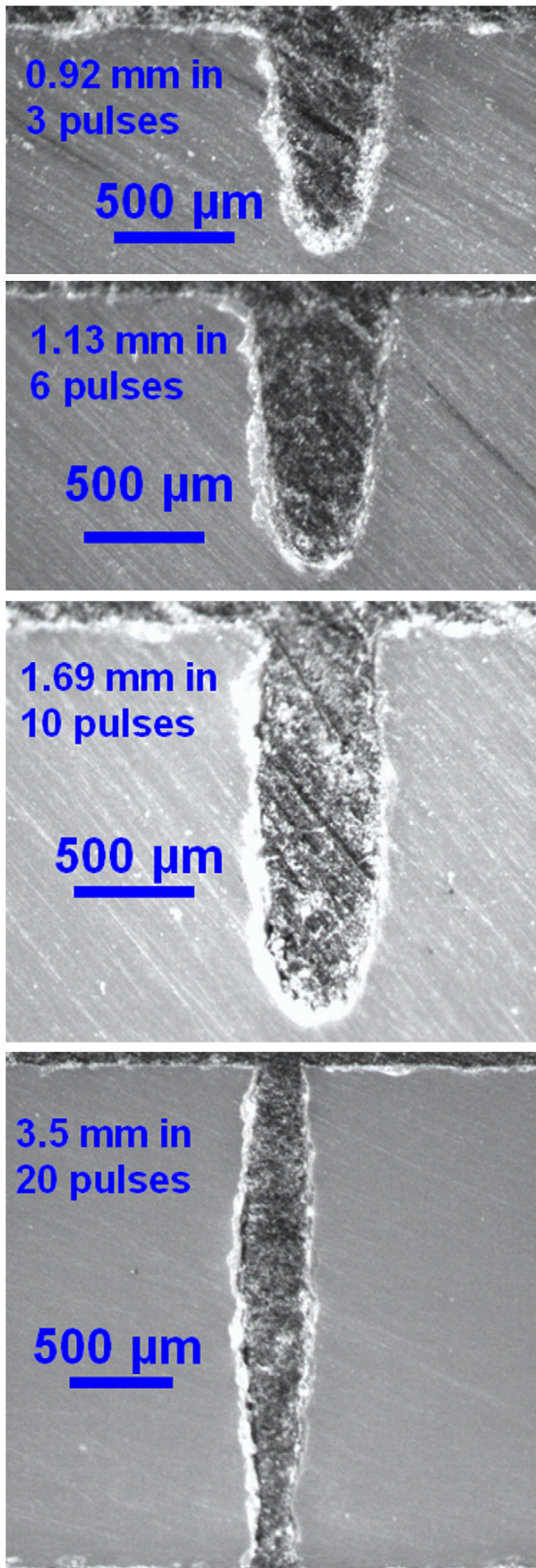

Fig. 26. Drilled holes in silicon nitride. (After Samant and Dahotre[62]).

CW CO_2 laser with a spot diameter of 2.7 mm was used by Firestone et al.[103] for the cutting process. The workpieces were initially heated to 1400 °C in a furnace to reduce the cracks and a gas jet minimized oxidation and plasma formation.[103] For SiC processed by KrF excimer lasers, ablation depth varied linearly with number of pulses and the surface showed flat as well as rough areas, debris deposit and thin scale formation.[92]

Three-dimensional contours have been made on SiC ceramic by a 450 W CW CO_2 laser by machining overlapping grooves for material removal. The grooves were formed by directing the beam tangential to the workpiece. Decreasing the groove depth on successive overlapping passes controlled the surface roughness of the finished components. This technique is similar to electrical-discharge machining and was used for generating flat or threaded surfaces on the workpiece.[108]

4.4. Aluminum nitride

Aluminum nitride (AlN) is commonly used in microelectronic substrates and packages because of its high thermal conductivity and small thermal expansion mismatch with silicon.[109] Lines and single – layer pockets were machined on AlN surface with an ultraviolet (UV) and near-infrared lasers and the effect of pulse overlap and pulse frequency on material removal rate and wall angle was predicted. However, there is no work reported that could explain the physical processes governing the machining in this ceramic. Maximum material removal rates (MRR) of 0.011 and 0.094 mm^3/s were achieved by UV and NIR lasers, respectively.[110] The steepest wall angle for an UV (Fig. 30a) and NIR laser (Fig. 30b) was 86° and 88°, respectively. Walls with steeper angles were produced at 95% overlap with NIR laser and at lower overlaps for UV laser.

Heat sinks were made out of AlN with laser machined cooling channels, the width and depth of which were controlled by

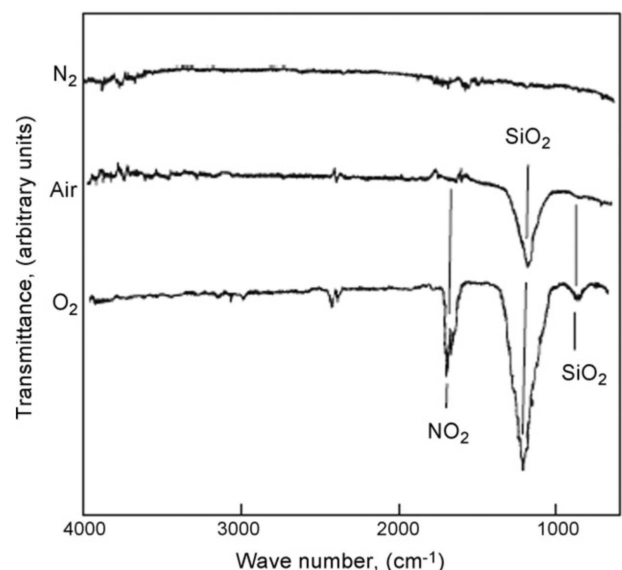

Fig. 27. Infrared absorption spectrum of atmosphere after laser machining of Si_3N_4. (After Shigematsu et al.[101] with kind permission of Springer Science + Business Media.)

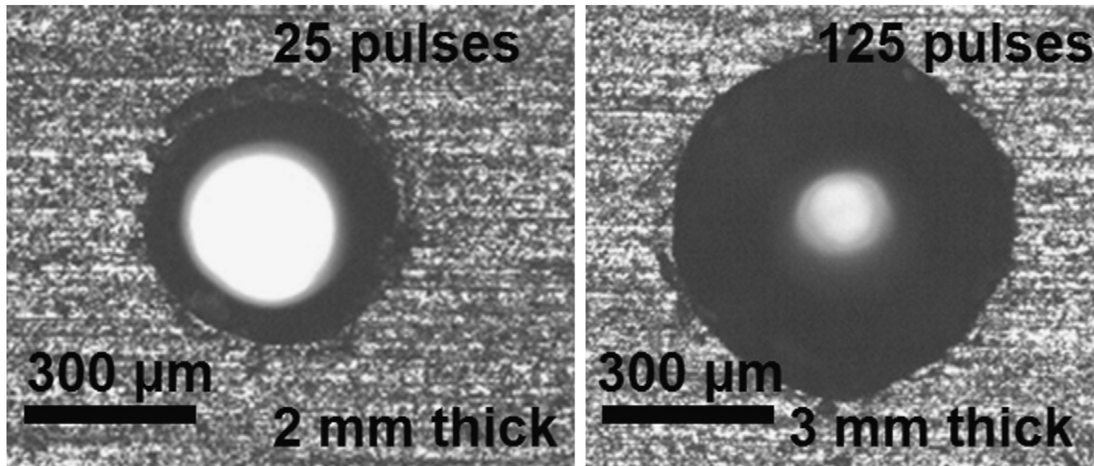

Fig. 28. Machining in 2 and 3 mm thick SiC plates. (After Samant et al.[66]).

the pulse width, the spot size and distance between the beam focus and the substrate. Laser energy of 7.5 J, pulse width of 0.9 ms, speed of 150 mm/min, and a pulse frequency of 60 Hz were used with nitrogen as a process gas for machining these

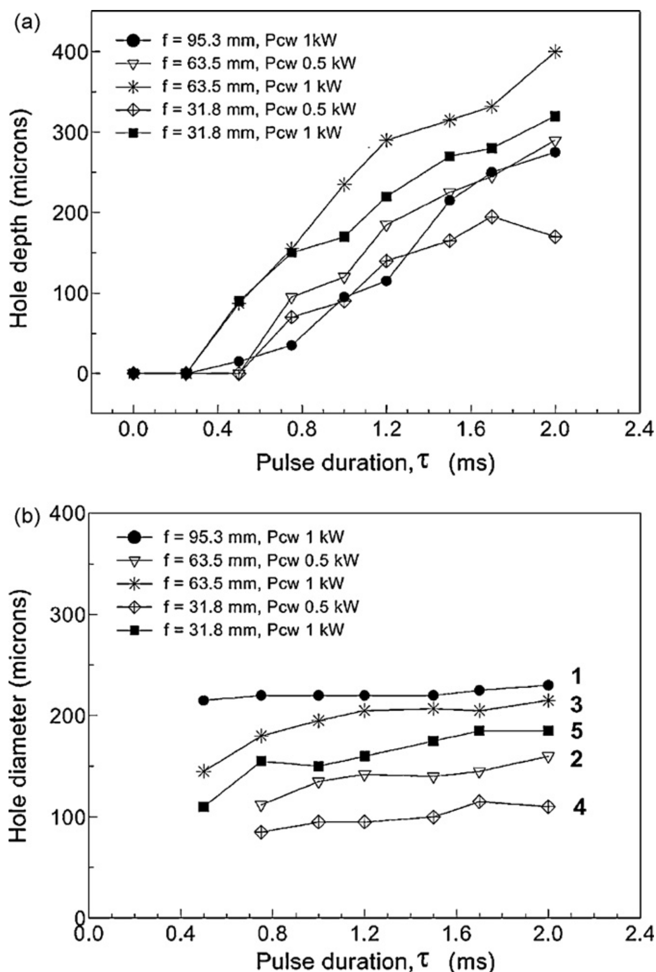

Fig. 29. Variation of (a) hole depth and (b) hole diameter with pulse duration for SiC drilling. (After Sciti and Bellosi[74] with permission. Copyright Elsevier.)

cooling channels.[91] A Lambda Physik LPX 210icc excimer laser was used for fabricating small diameter and high aspect ratio holes at designated locations in AlN ceramic. The ablation depth increased with decreasing pressure (Fig. 31a) and increasing fluence (Fig. 31b). The effective ablation rate saturated at high fluences due to attenuation by plasma and re-ablation of redeposited debris from earlier pulses. Plasma reduced the effective energy reaching the ceramic surface, thus removing less material per pulse. Also, redeposition generated an error in the depth measurement as the coating of the previously ablated material made the hole appear shallower.[109]

4.5. Zirconia

Low thermal conductivity, low coefficient of friction, excellent corrosion and wear resistance, high fracture toughness, and good thermal shock resistance make zirconia suitable for use in bearings, pH meters, fuel cells, infrared radiators, thread guides, pressure sensors, and oxygen sensors.[111] A pulsed Nd:YAG laser was used for drilling zirconia ceramic and the observations were input to MINITAB software for optimizing the parameters to obtain minimum heat-affected zone (HAZ) and taper. It was found that minimum HAZ thickness of 0.0675 mm (Fig. 32) could be obtained when the lamp current, pulse frequency, assisted air pressure, and pulse width are set at 17A, 2 kHz, 2 kg/cm^2 and 2% of the duty cycle, respectively. The corresponding optimum parameters to attain a minimum taper of 0.0319 were lamp current of 17 A, pulse frequency of 2 kHz, air pressure of 0.6 kg/cm^2 and pulse width of 2% of the duty cycle (Fig. 33).

Using a 10 kW Nd:YAG laser, at a power density of 5 MW/cm^2, 1.3 mm thick ZrO_2 samples were machined at 200 mm/min.[107] Laser cutting of magnesia-stabilized zirconia (PSZ) was also investigated using a 15 kW CW CO_2 laser by preheating at 660 and 957 °C with single and multiple passes. The power varied from 2 to 6 kW with cutting speeds varying from 9100 to 16,000 mm/min and the resultant depth of cut ranged from 0.13 to 0.9 mm.[103] ZrO_2 was machined by excimer

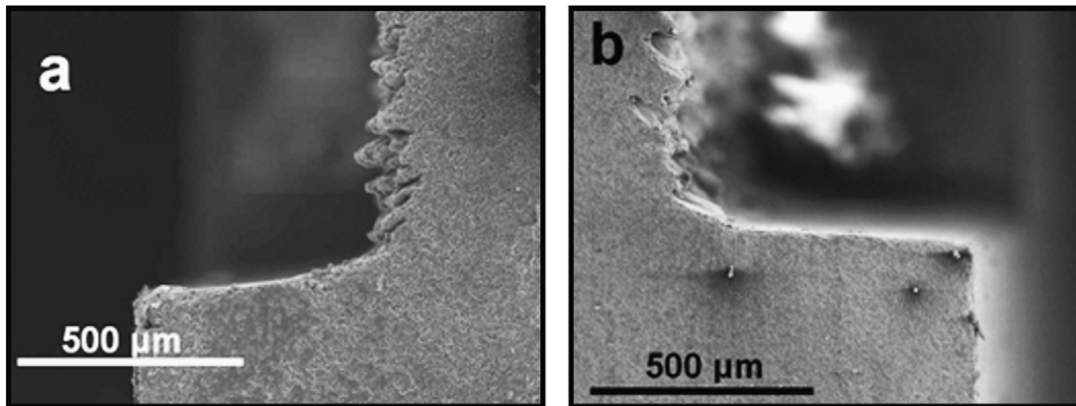

Fig. 30. Pocket edges machined in AlN with (a) UV laser with a 93% overlap and (b) NIR laser with a 95% overlap. (After Gilbert et al.[110] with permission. Copyright Elsevier.)

lasers and the mechanism for material removal was proposed to be melting and vaporization without the additional mechanism of dissociation that takes place in the case of SiC and Si_3N_4. Nevertheless, XeF laser machined surface demonstrated a porous structure and slower processing rate. ZrO_2 is transparent to 351 nm wavelength (wavelength of XeF laser) and the grain boundaries selectively absorbed the incident energy during laser processing. This selectively etched the grain boundaries and the processed surface appeared porous.[100]

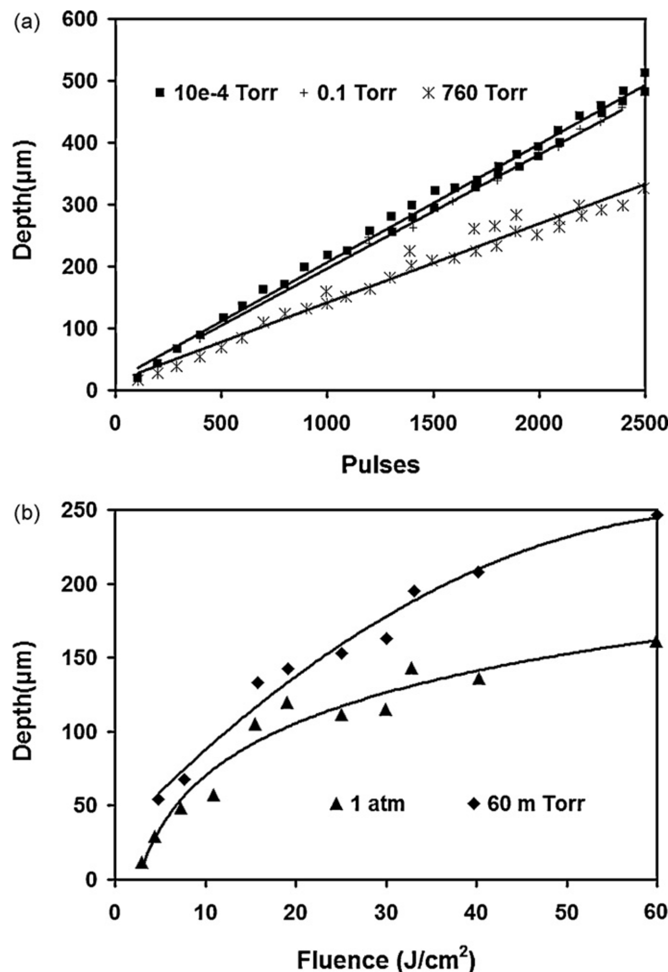

Fig. 31. (a) Variation of ablation depth with number of pulses at 40 J/cm^2 and for different pressures (b) variation of ablation depth with laser fluence at 60 mTorr and 760 Torr (1 atm).[109]

4.6. Magnesia

To the best of the present knowledge based on available literature, no significant work has been reported in the laser machining of pure MgO ceramic which has several industrial applications as mentioned earlier in this study. Samant and Dahotre have made an attempt in machining this ceramic with a pulsed Nd:YAG laser and the physical phenomena during the laser–ceramic interaction have been studied.[65] For pulse energy of 4 J, repetition rate of 20 Hz and pulse width of 0.5 ms, different number of pulses were applied to 3 mm thick MgO plates and the corresponding depth of the machined cavity was measured. Cavities that were 0.25, 0.86, 1.54 and 3 mm deep were formed when 3, 6, 9 and 20 pulses were incident on the ceramic. Instantaneous temperatures reached at the surface during laser machining are very high (higher than 2850 °C[116], the melting/decomposition/vaporization temperature of magnesia). At these high temperatures, magnesia dissociates as per the following reaction:[112,113]

$$\mathrm{MgO} \rightarrow \mathrm{Mg(s)} + \mathrm{O(g)} \quad (22)$$

The melting and vaporization temperatures of magnesium are 649 °C[114] and 1090 °C[115], respectively. The decomposition temperature of magnesia being much higher than both the melting and vaporization temperatures of magnesium, Mg(s) generated by the above reaction instantaneously vaporizes. Hence, at high temperatures reached during laser machining, the material losses in magnesia take place solely by the vaporization of magnesium. Thus, in MgO, the dissociation of the ceramic followed by evaporation is responsible for material removal.[65]

As the material evaporates, it exerts a force over the machined area and material removal takes place by corresponding pressure (vapor pressure) acting upwards and proportional to the laser fluence (input energy/beam cross-sectional area):

$$\text{Vapor pressure} = \frac{\text{laser fluence}}{\text{machined depth}} \quad (23)$$

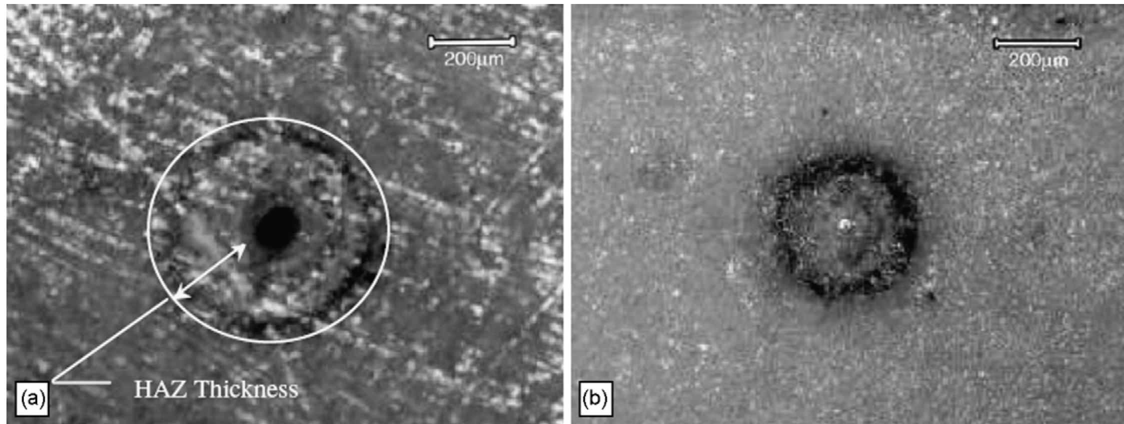

Fig. 32. Minimum HAZ thickness in ZrO_2: (a) top surface, (b) bottom surface. (After Kuar et al.[23] with permission. Copyright Elsevier.)

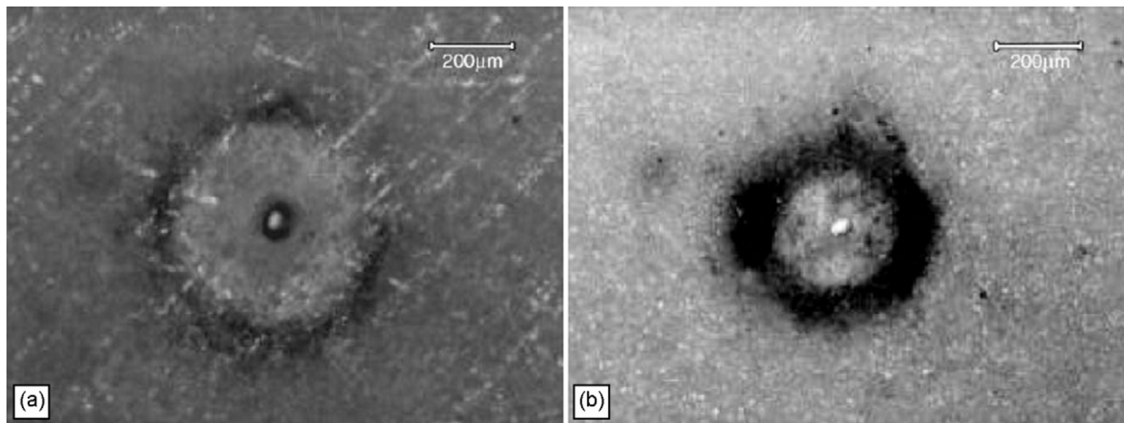

Fig. 33. Hole drilled in ZrO_2 with minimum taper: (a) top surface, (b) bottom surface. (After Kuar et al.[23] with permission. Copyright Elsevier.)

Moreover, the evaporated material is also subjected to gravitational pull acting downwards and given by ρgh, where ρ is density of the ceramic, g is the acceleration due to gravity (9.8 m/s^2) and h is the machined depth. The cavity formation is governed by the effect of these counteracting pressures (vapor pressure and gravitational pressure) and a clean cavity (Fig. 34) is formed when the vapor pressure exceeds the gravitational pressure.[65]

In addition to the above-mentioned illustrations, there would be several studies of laser machining of these and other structural ceramics. However, these few specific examples suffice the purpose of explaining the effects in laser machining of ceramics

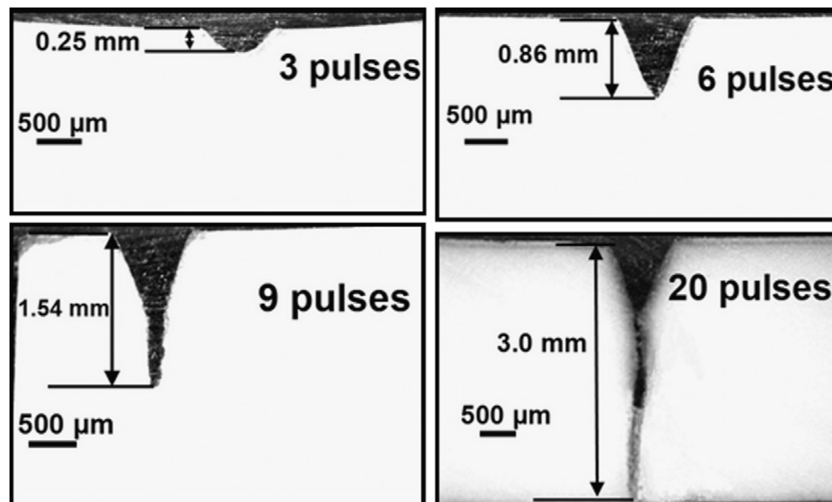

Fig. 34. Machining in MgO ceramic. (After Samant and Dahotre[65]).

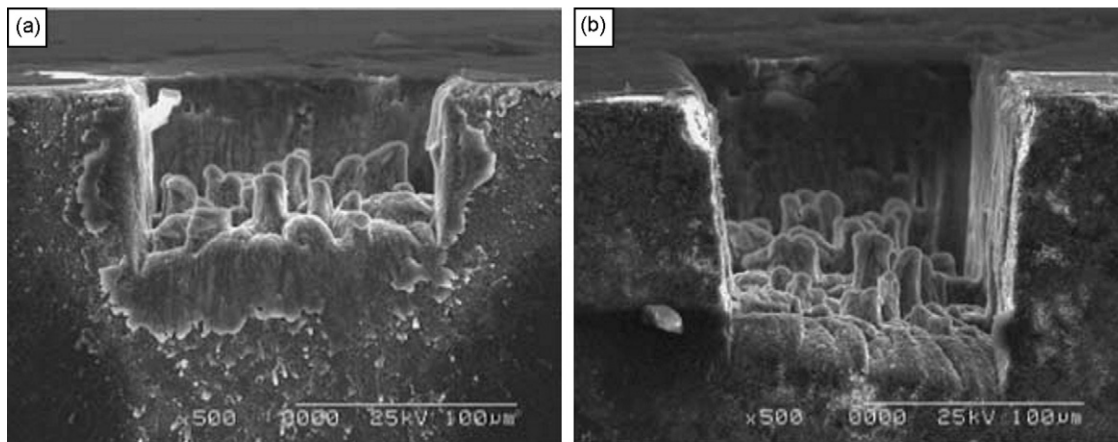

Fig. 35. Cross-section of craters formed in Al_2O_3–TiC after treatment at 10 J/cm^2 with (a) 500 and (b) 1000 laser pulses. (After Oliveira et al.[119] with kind permission of Springer Science + Business Media.)

based on combinations of various physical phenomena. Finally, the next section briefly looks at some of the recent advances in the field of laser micromachining.

5. Laser micromachining

There is an increasing demand for producing parts with micro and meso scale features in the field of semi-conductors, biomedical devices and optics.[117] In light of this demand, several techniques such as mechanical micromachining (micro-grooving, micro-milling), focused ion-beam micromachining, laser micromachining are being used in microfabrication. Laser micromachining is a comparatively new technique and provides improved flexibility in dimensional design of microproducts[49] and they can produce kerfs with depth and width smaller than 100 μm. Nd:YAG lasers are more widely used than CO_2 lasers because of their high energy density and small focused spot.[36] Material removal in laser micromachining mainly takes place by ablation and laser-assisted chemical etching. The growing demand for structural ceramics for different applications requires novel machining technologies with high accuracy and efficiency. Some work in the field of laser micromachining has been carried out by Oliveira et al.[118,119] who have machined Al_2O_3–34 wt.% TiC ceramics which are being increasingly used for high precision parts such as magnetic head sliders (Fig. 35).

However, no detailed studies on the physics behind laser micromachining of structural ceramics have been found in open literature. The common problems associated with conventional micromachining are tool wear and force-induced damage on ceramic components.[120] These problems can be adequately addressed by using thermal softening by a laser heat source during micro-machining. Thus, laser micro-machining of structural ceramics is still a gray area and has immense potential for research and applications.

6. Conclusion

In this study, an attempt has been made to cover the laser machining of several structural ceramics such as alumina, silicon nitride, silicon carbide, aluminum nitride, zirconia and magnesia after thoroughly understanding the physical phenomena associated with the machining process. The mechanism governing the material removal is a function of the material properties and the laser processing conditions. Laser micromachining of ceramics can also be used for producing parts at micro and meso scale. Overall, it seems that laser processing being a rapid, non-contact and flexible process, machining of structural ceramics by lasers is a budding field with tremendous applications in the future.

References

1. *New Structural Materials Technologies: Opportunities for the Use of Advanced Ceramics and Composites – A Technical Memorandum*, U.S. Congress, 1986.
2. Tuersley, I. P., Jawaid, A. and Pashby, I. R., Review: various methods of machining advanced ceramic materials. *J. Mater. Process. Technol.*, 1994, **42**(4), 377–390.
3. Schwartz, M., *Handbook of Structural Ceramics*, McGraw-Hill, New York, 1992, ISBN: 0070557195.
4. Vikulin, V., Kelina, I., Shatalin, A. and Rusanova, L., Advanced ceramic structural materials. *Refractories Ind. Ceram.*, 2004, **45**, 383–386.
5. Wang, H., Wang, C. A., Yao, X. and Fang, D., Processing and mechanical properties of zirconium diboride-based ceramics prepared by spark plasma sintering. *J. Am. Ceram. Soc.*, 2007, **90**, 1992–1997.
6. Kim, J. D., Lee, E. S. and Lee, C. Y., Crack generation and the effect of in-process electro-discharge dressing in grinding single crystal MgO. *Int. J. Mech. Sci.*, 1995, **37**, 569–583.
7. Kim, J. D. and Lee, E. S., A study on the mirror-like grinding of MgO single crystal with various diamond wheels. *J. Mater. Process. Technol.*, 1997, **72**, 1–10.
8. Kalpakjian, S. and Schmid, S. R., *Manufacturing Engineering and Technology*, Prentice Hall, Upper Saddle River, NJ, 2001, ISBN: 0201361310.
9. König, W. and Wagemann, A., Machining of ceramic components—process-technological potentials. *Machining Adv. Mater.*, 1993, **847**, 3–16 [NIST Special Publication].
10. Chryssolouris, G., Anifantis, N. and Karagiannis, S., Laser assisted machining: an overview. *J. Manuf. Sci. Eng.*, 1997, **119**(4B), 766–769.
11. Koepke, B. G. and Stokes, R. J., A study of grinding damage in magnesium oxide single crystals. *J. Mater. Sci.*, 1970, **5**(3), 240–247.
12. Kirchner, H. P., Damage penetration at elongated machining grooves in hot-pressed Si_3N_4. *J. Am. Ceram. Soc.*, 1984, **67**(2), 127–132.
13. Zhang, B., Precision grinding regime of advanced ceramics. In *Proceedings of Annual Meeting of American Society of Precision Engineering*, 1993, pp. 225–229.

14. Xu, H. H. K. and Jahanmir, S., Microfracture and material removal in scratching of alumina. *J. Mater. Sci.*, 1995, **30**(9), 2235–2247.
15. Zhang, B., Zheng, X. L., Tokura, H. and Yoshikawa, M., Grinding induced damage in ceramics. *J. Mater. Process. Technol.*, 2003, **132**, 353–364.
16. Thoe, T. B., Aspinwall, D. K. and Wise, M. L. H., Review on ultrasonic machining. *Int. J. Mach. Tools Manuf.*, 1998, **38**(4), 239–255.
17. Choi, J. P., Jeon, B. H. and Kim, B. H., Chemical-assisted ultrasonic machining of glass. *J. Mater. Process. Technol.*, 2007, **191**(1–3), 153–156.
18. Gudimetla, P., Wang, J. and Wong, W., Kerf formation analysis in the abrasive waterjet cutting of industrial ceramics. *J. Mater. Process. Technol.*, 2002, **128**(1–3), 123–129.
19. Park, J. M., Jeong, S. C., Lee, H. W., Jeong, H. D. and Lee, E., A study on the chemical mechanical micro-machining (C3M) process and its application. *J. Mater. Process. Technol.*, 2002, **130–131**, 390–395.
20. Puertas, I. and Luis, C. J., A study on the electrical discharge machining of conductive ceramics. *J. Mater. Process. Technol.*, 2004, **153–154**, 1033–1038.
21. Chak, S. K. and Rao, P. V., Trepanning of Al_2O_3 by electro-chemical discharge machining (ECDM) process using abrasive electrode with pulsed DC supply. *Int. J. Mach. Tools Manuf.*, 2007, **47**(14), 2061–2070.
22. Horio, K., Terabayashi, T. and Taniguchi, N., Beam defocus effect in electron beam machining of green ceramic sheet. *CIRP Ann. – Manuf. Technol.*, 1987, **36**(1), 95–98.
23. Kuar, A. S., Doloi, B. and Bhattacharyya, B., Modelling and analysis of pulsed Nd:YAG laser machining characteristics during micro-drilling of zirconia (ZrO_2). *Int. J. Mach. Tools Manuf.*, 2006, **46**(12–13), 1301–1310.
24. Jia, Z. X., Zhang, J. H. and Ai, X., High quality machining of engineering ceramics. *Key Eng. Mater.*, 1995, **108–110**, 155–164.
25. Shih, H. and Shu, K., A study of electrical discharge grinding using a rotary disk electrode. *Int. J. Adv. Manuf. Technol.*, 2008, **38**, 59–67.
26. Bäuerle, D., *Laser Processing and Chemistry*, Springer, New York, 2000, ISBN: 3540668918.
27. Lei, S., Shin, Y. C. and Incropera, F. P., Experimental investigation of thermo-mechanical characteristics in laser-assisted machining of silicon nitride ceramics. *J. Manuf. Sci. Eng.*, 2001, **123**, 639–646.
28. Rozzi, J. C., Pfefferkorn, F. E., Incropera, F. P. and Shin, Y. C., Transient, three-dimensional heat transfer model for the laser assisted machining of silicon nitride. I. Comparison of predictions with measured surface temperature histories. *Int. J. Heat Mass Transfer*, 2000, **43**(8), 1409–1424.
29. Rozzi, J. C., Pfefferkorn, F. E., Incropera, F. P. and Shin, Y. C., Transient thermal response of a rotating cylindrical silicon nitride workpiece subjected to a translating laser heat source. Part I. Comparison of surface temperature measurements with theoretical results. *J. Heat Transfer*, 1998, **120**, 899–906.
30. Rozzi, J. C., Incropera, F. P. and Shin, Y. C., Transient thermal response of a rotating cylindrical silicon nitride workpiece subjected to a translating laser heat source. Part II. Parametric effects and assessment of a simplified model. *J. Heat Transfer*, 1998, **120**, 907–915.
31. Rozzi, J. C., Incropera, F. P. and Shin, Y. C., Transient, three-dimensional heat transfer model for the laser assisted machining of silicon nitride. II. Assessment of parametric effects. *Int. J. Heat Mass Transfer*, 2000, **43**(8), 1425–1437.
32. Lei, S., Shin, Y. C. and Incropera, F. P., Deformation mechanisms and constitutive modeling for silicon nitride undergoing laser-assisted machining. *Int. J. Mach. Tools Manuf.*, 2000, **40**(15), 2213–2233.
33. Pfefferkorn, F. E., Shin, Y. C., Tian, Y. and Incropera, F. P., Laser-assisted machining of magnesia-partially-stabilized zirconia. *J. Manuf. Sci. Eng.*, 2004, **126**, 42–51.
34. Chang, C. W. and Kuo, C. P., An investigation of laser-assisted machining of Al_2O_3 ceramics planning. *Int. J. Mach. Tools Manuf.*, 2007, **47**(3–4), 452–461.
35. www.lasercheval.fr/eng/subcontracting.php.
36. Chryssolouris, G., *Laser Machining Theory and Practice*. Springer-Verlag, New York, 1991.
37. Albright, C., *Laser Welding, Machining and Materials Processing*. IFS (Publications) Ltd. and Springer-Verlag, New York, 1985.
38. Pandey, P. C. and Shan, H. S., *Modern Machining Processes*. McGraw Hill, New Delhi, 1980.
39. Sun, S., Durandet, Y. and Brandt, M., Parametric investigation of pulsed Nd:YAG laser cladding of stellite 6 on stainless steel. *Surf. Coat. Technol.*, 2005, **194**(2–3), 225–231.
40. Islam, M. U. and Campbell, G., Laser machining of ceramics: A review. *Mater. Manuf. Processes*, 1993, **8**(6), 611–630.
41. Ki, H., Mohanty, P. S. and Mazumder, J., Multiple reflection and its influence on keyhole evolution. *J. Laser Appl.*, 2002, **14**, 39–45.
42. Bang, S. Y. and Modest, M. F., Multiple reflection effects on evaporative cutting with a moving CW laser. *J. Heat Transfer*, 1991, **113**, 663–669.
43. Zhao, J., *Numerical Simulation of High Intensity Laser Drilling of Metals*. Masters Thesis. The University of Tennessee, Knoxville, TN, 1999.
44. Minamida, K., Takafuji, H., Hamada, N., Haga, H. and Mizuhashi, N., Wedge shape welding with multiple reflection effects of high power CO_2 laser beam. In *Proceedings of the 5th Int. Congress on Applications of Lasers and Electro-optics*, 1986, pp. 97–104.
45. Rahman, F. A., Takahashi, K. and Teik, C. H., Theoretical analysis of coupling between laser diodes and conically lensed single-mode fibres utilising ABCD matrix method. *Opt. Commun.*, 2003, **215**(1–3), 61–68.
46. Bang, S. Y., Roy, S. and Modest, M. F., CW laser machining of hard ceramics-II. Effects of multiple reflections. *Int. J. Heat Mass Transfer*, 1993, **36**(14), 3529–3540.
47. Modest, M. F., Effects of multiple reflections on hole formation during short-pulsed laser drilling. *J. Heat Transfer*, 2006, **128**(7), 653–661.
48. Baily, A. W. and Modak, A., Numerical simulation of laser ablation with cavity reflections. *J. Thermophys. Heat Transfer*, 1989, **3**, 42–45.
49. Dahotre, N. B. and Harimkar, S. P., *Laser Fabrication and Machining of Materials*. Springer, New York, NY, 2008.
50. Andrews, J. G. and Atthey, D. R., Hydrodynamic limit to penetration of a material by a high-power beam. *J. Phys. D: Appl. Phys.*, 1976, **9**, 2181–2194.
51. Mazumdar, J. and Steen, W. M., Heat transfer model for CW laser material processing. *J. Appl. Phys.*, 1980, **51**, 941.
52. Steen, W. M., *Laser Materials Processing*. Springer, London, 1991.
53. Dubey, A. K. and Yadava, V., Experimental study of Nd:YAG laser beam machining—An overview. *J. Mater. Process. Technol.*, 2008, **195**(1–3), 15–26.
54. Salonitis, K., Stournaras, A., Tsoukantas, G., Stavropoulos, P. and Chryssolouris, G., A theoretical and experimental investigation on limitations of pulsed laser drilling. *J. Mater. Process. Technol.*, 2007, **183**(1), 96–103.
55. Morita, N., Ishida, S., Fujimori, Y. and Ishikawa, K., Pulsed laser processing of ceramics in water. *Appl. Phys. Lett.*, 1988, **52**(23), 1965–1966.
56. Kovalenko, V. S. and Laurinovich, A. V., Laser machining of ceramic materials. In *Proceedings of 6th Int. Conf. on Production Engineering*, 1987, pp. 627–631.
57. Kim, M. J., 3D Finite element analysis of evaporative laser cutting. *Appl. Math Model.*, 2005, **29**(10), 938–954.
58. Kim, M. J. and Zhang, J., Finite element analysis of evaporative cutting with a moving high energy pulsed laser. *Appl. Math Model.*, 2001, **25**(3), 203–220.
59. Modest, M. F. and Abakian, H., Heat conduction in a moving semi-infinite solid subjected to pulsed laser irradiation. *ASME J. Heat Transfer*, 1986, **108**, 602–607.
60. Abakian, H. and Modest, M. F., Evaporative cutting of a semi-transparent body with a moving CW laser. *ASME J. Heat Transfer*, 1988, **110**, 924–930.
61. Modest, M., Laser machining of ablating/decomposing materials through cutting and drilling models. *J. Laser Appl.*, 1997, **9**, 137–145.
62. Samant, A. N. and Dahotre, N. B., Ab initio physical analysis of single dimensional laser machining of silicon nitride. *Adv. Eng. Mater.*, 2008, **10**, 978–981.
63. Samant, A. N. and Dahotre, N. B., Computational predictions in single dimensional laser machining of alumina. *Int. J. Mach. Tools Manuf.*, 2008, **48**, 1345–1353.
64. Samant, A. N. and Dahotre, N. B., Differences in physical phenomena governing laser machining of structural ceramics. *Ceram. Int.*, in press, corrected proof, doi:10.1016/j.ceramint.2008.11.013.

65. Samant, A. N. and Dahotre, N. B., An integrated computational approach to single dimensional laser machining of magnesia. *Opt. Lasers Eng.*, in press, corrected proof, doi:10.1016/j.optlaseng.2008.10.001.
66. Samant, A. N., Daniel, C., Chand, R. H., Blue, C. A. and Dahotre, N. B., Computational approach to photonic drilling of silicon carbide. *Int. J. Adv. Manuf. Technol*., under review.
67. Semak, V. V., Knorovsky, G. A., MacCallum, D. O. and Roach, R. A., Effect of surface tension on melt pool dynamics during laser pulse interaction. *J. Phys. D: Appl. Phys.*, 2006, **39**, 590–595.
68. Semak, V. V., Knorovsky, G. A. and MacCallum, D. O., On the possibility of microwelding with laser beams. *J. Phys. D: Appl. Phys.*, 2003, **36**, 2170–2174.
69. Anisimov, S. I., Vaporization of metal absorbing laser radiation. *Sov. Phys. JETP*, 1968, **27**, 182–183.
70. Tönshoff, H. K. and Kappel, H., Surface modification of ceramics by laser machining. *CIRP Ann. – Manuf. Technol.*, 1998, **47**(1), 471–474.
71. Tönshoff, H. K., Hesse, D. and Gonschior, M., Microstructuring with excimer lasers and reduction of deposited ablation products using a special gas nozzle with a vacuum system. In *Proceedings of ICALEO*, 1994, pp. 333–342.
72. Islam, M. U., An overview of research in the fields of laser surface modification and laser machining at the Integrated Manufacturing Technologies Institute, NRC. *Adv. Perform. Mater.*, 1996, **3**, 215–238.
73. Laude, L. D., Ogeret, C., Jadin, A. and Kolev, K., Excimer laser ablation of Y-SiAlON. *Appl. Surf. Sci.*, 1998, **127–129**, 848–851.
74. Sciti, D. and Bellosi, A., Laser-induced surface drilling of silicon carbide. *Appl. Surf. Sci.*, 2001, **180**, 92–101.
75. Dubey, A. K. and Yadava, V., Optimization of kerf quality during pulsed laser cutting of aluminium alloy sheet. *J. Mater. Process. Technol.*, 2008, **204**(1–3), 412–418.
76. Tsai, C. H. and Chen, H. W., Laser cutting of thick ceramic substrates by controlled fracture technique. *J. Mater. Process. Technol.*, 2003, **136**(1–3), 166–173.
77. Liu, J. S., Li, L. J. and Jin, X. Z., Accuracy control of three-dimensional Nd:YAG laser shaping by ablation. *Opt. Laser Technol.*, 1999, **31**, 419–423.
78. Perrie, W., Rushton, A., Gill, M., Fox, P. and O'Neill, W., Femtosecond laser micro-structuring of alumina ceramic. *Appl. Surf. Sci.*, 2005, **248**(1–4), 213–217.
79. Longfellow, J., High speed drilling in alumina substrates with a CO_2 laser. *Am. Ceram. Soc. Bull.*, 1971, **50**(3), 251–253.
80. Saifi, M. A. and Borutta, R., Optimization of pulsed CO_2 laser parameters for Al_2O_3 scribing. *Ceram. Bull.*, 1975, **54**, 986–989.
81. Ananthapadmanabhan, P. V., Thiyagarajan, T. K., Sreekumar, K. P. and Venkatramani, N., Formation of nano-sized alumina by in-flight oxidation of aluminium powder in a thermal plasma reactor. *Scr. Mater.*, 2004, **50**(1), 143–147.
82. Wagner, R. E., Laser drilling mechanics. *J. Appl. Phys.*, 1974, **45**(10), 4631–4637.
83. Coherent, Inc., *Lasers-Operation, Equipment, Application, and Design*, McGraw Hill, New York, 1980.
84. Chryssolouris, G. and Bredt, J., Machining of ceramics using a laser lathe. In *Proceedings of Intersociety Symp. on Machining of Adv. Ceram. Mater. and Components*, ed. R. E. Barks, K. Subramanian, and K. E. Ball, Pittsburgh, PA, 1987, pp. 70–72.
85. Hamann, C. and Rosen, H., Laser machining of ceramic and silicon. *Industrial Laser Annal Handbook*. Penwell Pub., Tulsa, OK, 1986.
86. Tönshoff, H. K. and Emmelmann, E., *Laser Processing of Ceramics*. International Power Beam Conference, San Diego, CA, 1988.
87. Tönshoff, H. K. and Semrau, H., Laser beam machining in new fields of application. In *Conference on Research and Technology Development in Non-Traditional Machining*, 1988.
88. Tönshoff, H. K., Butje, R., Konig, W. and Trasser, F. J., Excimer laser in material processing. *Ann. CIRP*, 1988, **37**(2), 681–684.
89. Tönshoff, H. K. and Emmelmann, E., Laser cutting of advanced ceramics. *Ann. CIRP*, 1989, **38**(1), 219–222.
90. Guo, D., Cai, K., Yang, J. and Huang, Y., Spatter-free laser drilling of alumina ceramics based on gelcasting technology. *J. Eur. Ceram. Soc.*, 2003, **23**(8), 1263–1267.
91. Glaw, V., Hahn, R., Paredes, A., Hein, U., Ehrmann, O. and Reichl, H., Laser machining of ceramics and silicon for MCM-D applications. In *Proceedings of the 3rd International Symposium on Adv. Packaging Mater*, 1997, pp. 173–176.
92. Sciti, D., Melandri, C. and Bellosi, A., Excimer laser-induced microstructural changes of alumina and silicon carbide. *J. Mater. Sci.*, 2000, **35**, 3799–3810.
93. Wang, C. and Zeng, X., Study of laser carving three-dimensional structures on ceramics: quality controlling and mechanisms. *Opt. Laser Technol.*, 2007, **39**(7), 1400–1405.
94. Kelly, A. and Macmillan, N. H., *Strong Solids*. Oxford University Press, New York, 1986.
95. Wachtman, J. B., *Mechanical Properties of Ceramics*. John Wiley & Sons, New York, 1996.
96. Harrysson, R. and Herbertsson, H., Machining of high performance ceramics and thermal etching of glass by laser. In *Proceedings of the 4th International Conference on Lasers in Manufacturing*, 1987, pp. 211–219.
97. Murray, J. P., Flamant, G. and Roos, C. J., Silicon and solar-grade silicon production by solar dissociation of Si_3N_4. *Sol. Energy*, 2006, **80**(10), 1349–1354.
98. Copley, S. M., Laser shaping of materials. In *Proceedings of ASM Conference on Lasers in Materials Processing*, 1983, pp. 82–92.
99. Copley, S. M., Shaping ceramics with lasers. *Interdisciplinary Issues Mater Process. Manuf.*, 1987, 631.
100. Miyamoto, I. and Marou, H., Processing of ceramics by excimer lasers. *SPIE-Laser Assist. Process. II*, 1990, **1279**, 66.
101. Shigematsu, I., Kanayama, K., Tsuge, A. and Nakamura, M., Analysis of constituents generated with laser machining of Si_3N_4 and SiC. *J. Mater. Sci. Lett.*, 1998, **17**, 737–739.
102. Yamamoto, J. and Yamamoto, Y., Laser machining of silicon nitride. In *Proceedings of LAMP' 87*, 1987, p. 297.
103. Firestone, R. F. and Vesely Jr., E. J., High power laser beam machining of structural ceramics. In *Proceedings of the ASME Symposium on Machining of Adv. Ceram. Mater. & Components*, 1988, pp. 215–227.
104. Lavrinovich, A. V., Kryl, Y. A., Androsov, I. M. and Artemyuk, S. A., Effect of dimensional laser machining on the structure and properties of silicon nitride. *Powder Metall. Met. Ceram.*, 1990, **29**(4), 328–332.
105. Pham, D. T., Dimov, S. S. and Petkov, P. V., Laser milling of ceramic components. *Int. J. Mach. Tools Manuf.*, 2007, **47**(3–4), 618–626.
106. Polk, D. H., Banas, C. M., Frye, R. W. and Gragosz, R. A., Laser processing of materials. *Ind. Heat Exchangers*, 1986, 357–364.
107. Affolter, P. and Schmid, H. G., Processing of new ceramic materials with solid state laser radiation. *SPIE-High Power Lasers Ind. Appl.*, 1987, **801**, 120–129.
108. Copley, S., Bass, M., Jau, B. and Wallace, R., Shaping materials with lasers. *Laser Mater. Proc.*, 1983, 297–336.
109. Lumpp, K., Excimer laser machining and metallization of vias in aluminium nitride. *Mater. Sci. Eng., B*, 1997, **45**(1–3), 208–212.
110. Gilbert, T., Krstic, V. D. and Zak, G., Machining of aluminium nitride with ultra-violet and near-infrared Nd:YAG lasers. *J. Mater. Process. Technol.*, 2007, **189**(1–3), 409–417.
111. Liang, X. Y. and Dutta, S. P., Application trend in advanced ceramic technologies. *Technovation*, 2001, **21**, 61–65.
112. Yabe, T., Mohamed, M. S., Uchida, S., Baasandash, C., Sato, Y., Tsuji, M. and Mori, Y., Noncatalytic dissociation of MgO by laser pulses towards sustainable energy cycle. *J. Appl. Phys.*, 2007, **101**, 123106 –1-7, doi:10.1063/1.2743730.
113. Brewer, L. and Porter, R. F., A thermodynamic and spectroscopic study of gaseous magnesium oxide. *J. Chem. Phys.*, 1954, **22**, 1867–1877.
114. Weimin, Z., Yong, S., Haipeng, L. and Chunyong, L., The effects of some elements on the igniting temperature of magnesium alloys. *Mater. Sci. Eng.: B*, 2006, **127**(2–3), 105–107.
115. Massalski, T. B., Okamoto, H., Subramanian, P. R. and Kacprzak, L., *Binary Alloy Phase Diagrams*. ASM International, Materials Park, OH, 1990.
116. Bhushan, B. and Gupta, B. K., *Handbook of Tribology (Materials, Coatings and Surface Treatments)*. Mc Graw Hill, New York, 1991.

117. Singh, R., Alberts, M. J. and Melkote, S. N., Characterization and prediction of the heat-affected zone in a laser-assisted mechanical micromachining process. *Int. J. Mach. Tools Manuf.*, 2008, **48**(9), 994–1004.
118. Oliveira, V., Vilar, R., Conde, O. and Freitas, P., Laser micromachining of Al_2O_3 – TiC ceramic. *J. Mater. Res.*, 1997, **12**(12), 3206–3209.
119. Oliveira, V., Simoes, F. and Vilar, R., Column-growth mechanisms during KrF laser micromachining of Al_2O_3–TiC ceramics. *Appl. Phys. A*, 2005, **81**, 1157–1162.
120. Chen, T. C. and Darling, R. B., Laser micromachining of the materials using in microfluidics by high precision pulsed near and mid-ultraviolet Nd:YAG lasers. *J. Mater. Process. Technol.*, 2008, **98**, 248–253.